CD8$^+$ T cell recall cytotoxicity during chronic treated HIV-1 infection is associated with limited reservoir size and activity

David R. Collins[1,*], Mpho J. Olatotse[1], Jonathan M. Urbach[1], Zhu Zhuo[2], Suhui Zhao[3], Tyler J. Lilie[3], Rachel Raymond[3], Xianbao He[4], James Y. Chen[1], Bridget Coffey[1], Umar Arshad[1], Zachary J. Racenet[1], Hannah Wisner[1], Carlos Casquero[1], Xuan Guo[1], Lucy C. Walters[1], Jennifer M. Davis[5], Hannah C. Jordan[3], Noor Sohail[2], Kiera L. Clayton[6], Manish Sagar[4], James Billingsley[2], Shannan Ho Sui[2], Emanuele Mazzola[7], Bruce D. Walker[1,8,9,10], Athe Tsibris[3,10,*]

[1] Ragon Institute of Mass General Brigham, MIT and Harvard; Cambridge, MA, USA
[2] Harvard Chan Bioinformatics Core, Harvard T.H. Chan School of Public Health, Boston, MA, USA
[3] Division of Infectious Diseases, Brigham and Women's Hospital; Boston, MA, USA
[4] Department of Medicine, Boston Medical Center, Boston University Chobanian & Avedisian School of Medicine; Boston, MA, USA
[5] Division of Infectious Diseases, University of Nebraska Medical Center; Omaha, NE, USA
[6] Department of Pathology, University of Massachusetts Chan Medical School, Worcester, MA, USA
[7] Department of Data Science, Dana-Farber Cancer Institute; Boston, MA, USA
[8] Howard Hughes Medical Institute; Chevy Chase, MD, USA
[9] Institute for Medical Engineering and Sciences and Department of Biology, Massachusetts Institute of Technology; Cambridge, MA, USA
[10] Harvard Medical School; Boston, MA, USA
*Corresponding authors. Email: drcollins@mgh.harvard.edu; atsibris@bwh.harvard.edu

One Sentence Summary: CD8$^+$ T cell recall cytotoxicity against autologous HIV-1 epitopes associates with smaller and less transcriptionally active proviral reservoirs during prolonged antiretroviral therapy initiated during chronic infection.

Abstract: The combination of replication-competent HIV-1 proviral persistence and virus-specific immune dysfunction prevents virus clearance during antiretroviral therapy (ART), resulting in rebound viremia after treatment interruption. Functional impairment of HIV-specific CD8$^+$ T cells during chronic infection is typically not reversed by ART but has recently been shown to improve in some individuals after prolonged treatment. To evaluate the impact of cellular immune function on viral persistence, we mapped and functionally characterized HIV-1 epitope-specific CD8$^+$ T cell responses and virus reservoirs in sixty people with HIV-1 (PWH) who initiated prolonged ART during chronic progressive infection. In 17% of participants, recall cytotoxicity of proliferative CD8$^+$ T cells targeting one or more autologous proviral epitopes was comparable to responses in spontaneous HIV-1 controllers. These responses were associated with smaller and less transcriptionally active HIV-1 reservoirs during prolonged ART. Treatment interruption in one participant with moderately high HIV-specific CD8$^+$ T cell proliferative and cytolytic capacity resulted in a rapid reduction of rebound viremia coincident with *in vivo* HIV-specific CD8$^+$ T cell expansion and secondary cytotoxic effector cell differentiation. Collectively, these results highlight a potential role for recall cytotoxicity in limiting HIV-1 persistence during ART and attenuating rebound viremia after treatment interruption, which may inform strategies to elicit durable post-ART immune control.

INTRODUCTION

Cellular immune responses fail to control or eliminate infection in most people with HIV-1 (PWH) due to functional impairment of virus-specific $CD8^+$ T cells and mutational escape from recognition (*1*). In contrast, durable spontaneous control of HIV-1 infection is rare and is associated with proliferative and cytolytic $CD8^+$ T cell responses against non-escaped autologous viral epitopes (*2-7*). Initiation of antiretroviral therapy (ART) during the chronic phase of HIV-1 infection typically fails to reverse functional impairment of virus-specific $CD8^+$ T cells (*8*). However, ART initiation during very early stages of HIV-1 infection has been shown to preserve HIV-specific $CD8^+$ T cell proliferative capacity and memory formation (*9, 10*). Early ART initiation is also associated with smaller persistent proviral reservoirs (*11-15*) and a higher likelihood of post-treatment control of viremia (*16-19*). Recent evidence suggests that long-term ART can replenish HIV-specific $CD8^+$ T cell functionality to some extent (*20*), and emerging evidence suggests that functional $CD8^+$ T cells contribute to control of HIV-1 following combination immunotherapy (*21-23*). However, because most PWH fail to control viremia after treatment interruption, the extent to which HIV-specific $CD8^+$ T cells may contribute to suppression of persistent viral reservoirs during ART and of recrudescent viremia after ART is discontinued remain unclear.

We examined virus-specific $CD8^+$ T cell specificity, functionality, HIV-1 reservoir size, and treatment history in a cohort of 60 virologically suppressed PWH on prolonged ART that was initiated during chronic progressive HIV-1 infection. HIV-specific $CD8^+$ T cells from most participants were nonproliferative or failed to recognize autologous proviral epitopes due to mutational escape. However, HIV-specific $CD8^+$ T cells in a subset of individuals maintained high proliferative and cytolytic potential against autologous proviral epitopes, comparable to responses in durable spontaneous HIV-1 controllers. Relative to participants with poorly functional and/or mutationally escaped $CD8^+$ T cells, participants with highly functional, non-escaped responses harbored less total and intact HIV-1 DNA and significantly less cell-associated HIV-1 RNA among $CD4^+$ T cells. We characterized longitudinal immune responses in one participant who underwent ART interruption while viremia was monitored. Plasma viremia rebounded after two weeks but rapidly declined concurrently with *in vivo* expansion and cytolytic differentiation of HIV-specific $CD8^+$ T cells. These results demonstrate that HIV-specific $CD8^+$ T cells with preserved cytolytic recall potential exist in a subset of PWH treated during chronic infection. Their association with smaller HIV-1 reservoirs during ART and rapid reduction of viremia following ART interruption highlights the promise of inducing such responses in prospective HIV-1 cure approaches.

RESULTS

Some $CD8^+$ T cells retain proliferative capacity against autologous HIV-1 during ART

HIV-1 epitope-specific $CD8^+$ T cell responses were mapped using peripheral blood mononuclear cells (PBMCs) obtained from sixty PWH enrolled in the HIV Eradication and Latency (HEAL) study. All participants had initiated therapy during chronic progressive infection (median CD4 nadir 206 cells/mm^3) and remained on ART for a minimum of one year (median 19 years) prior to sampling (Table 1). This study population was not enriched for protective or risk HLA genotypes known to have strong associations with viral load setpoint (*24, 25*) (Fig. S1A, Data file S1). HIV epitope-specific $CD8^+$ T cell responses were mapped using interferon-γ (IFN-γ)

enzyme-linked immunospot (elispot) following overnight stimulation with an array of individual HLA-optimal subtype B consensus HIV-1 peptides matched for each participant's HLA genotype (Fig. 1A). 221 responses of varying magnitude were detected across 60 participants, with a median of 3 and a range of 0 to 18 epitope-specific responses per participant (Fig. 1B-C).

We next assessed HIV-specific $CD8^+$ T cell functionality by measuring HIV-1 epitope-specific $CD8^+$ T cell proliferation via CFSE dilution in response to six-day peptide stimulation (Fig. 1D). The proliferative capacity of most HIV-specific responses detected by elispot was severely impaired, with only a modest correlation between IFN-γ production and proliferation (Fig. 1E). However, 21 (9.5%) of 221 HIV-1 epitope-specific responses from 17 of 60 HEAL participants exhibited unexpectedly high proliferative capacity (≥5% CFSE dilution), compared to 15 (27%) of 55 responses from 8 of 10 spontaneous HIV-1 controllers in a separate cohort (Fig. S1B-D).

To examine whether these highly proliferative responses recognized all cognate epitope variants present within autologous HIV-1 proviruses, we sequenced targeted epitopes within proviral DNA using nested PCR of segmented amplicons from $CD4^+$ T cells and then measured degranulation and cytokine production in response to stimulation with peptides matching each autologous epitope sequence observed (Fig. 1F). Analysis of proviral sequences revealed autologous variants relative to the clade B consensus epitopes detected within 13 of the 21 observed highly proliferative responses. Of these, 8 were cross-recognized and 5 had escaped from recognition, totaling 16 non-escaped, highly proliferative responses from 14 participants (Fig 1G). These results identified a subset of PWH with highly proliferative $CD8^+$ T cell responses to autologous proviral epitopes following prolonged ART initiated during chronic progressive infection.

Proliferative HIV-specific $CD8^+$ T cells durably maintain high recall cytotoxicity

Using an expanded antigen-specific elimination assay (*26*), we next measured the capacity of immunodominant HIV-1 epitope-specific $CD8^+$ T cells to kill autologous peptide-pulsed $CD4^+$ T cells after a six-day *in vitro* re-exposure to antigen (Fig. 2A). Proliferative responses exhibited higher recall cytotoxicity than nonproliferative responses (Fig. 2B) and we observed a strong positive correlation between proliferation and recall cytotoxicity (Fig. 2C). Of the 16 non-escaped highly proliferative responses we observed from 14 participants, 11 proliferative responses from 10 participants (17% of the cohort) demonstrated high recall cytotoxicity (area under the curve (AUC) >100), comparable to or higher than the first quartile of immunodominant $CD8^+$ T cell responses from spontaneous controllers (Fig. S1E). Responses in HEAL participants with high proliferation and recall cytotoxicity were not unique in their HLA restriction or HIV-1 protein/epitope targeting (Fig. S1F-G, Data file S1).

Using specimens obtained over time (median 2.6 years, range 0.7-4.9 years) during continuous ART from 7 participants with high recall cytotoxicity and available longitudinal samples, we also assessed the extent to which the cytolytic potential of these responses was durably maintained. HIV-specific $CD8^+$ T cell recall cytotoxicity remained high in all participants (Fig. 2D). In addition, proliferative $CD8^+$ T cell responses from HEAL participants were capable of killing HIV-infected cells presenting naturally processed viral epitopes comparably to responses from spontaneous HIV-1 controllers (Fig. S2). These results demonstrate that individuals with

highly proliferative HIV-1 epitope-specific $CD8^+$ T cell responses also durably maintain high cytotoxic recall potential against HIV-infected cells during ART.

HIV-specific $CD8^+$ T cells with differing functionality are phenotypically similar
To investigate relationships between the functionality, frequency, and phenotype of virus-specific $CD8^+$ T cells among PWH treated during chronic infection, we profiled immunodominant HIV-1 epitope-specific $CD8^+$ T cells *ex vivo* using peptide-HLA (pHLA) tetramers. Although large responses were frequently nonproliferative (Fig. 1E), highly proliferative HIV-1 epitope-specific $CD8^+$ T cells were typically present at higher *ex vivo* frequencies than nonproliferative cells (Fig. S3A), suggesting that functional HIV-specific $CD8^+$ T cells are generally more expanded *in vivo*, consistent with their capacity to further expand and differentiate into cytotoxic effector cells *in vitro*. However, phenotypic analysis revealed no consistent differences between highly and poorly functional responses in memory, activation, or differentiation states as defined by *ex vivo* staining for CD45RA, CD62L, CD38, PD-1, CD127, granzyme B, or TCF-1 (Fig. S3B-G). These results indicate that superior $CD8^+$ T cell responsiveness is not associated with reduced markers of immune activation or exhaustion. That these phenotypic markers were insufficient to predict functionality underscores the importance of *in vitro* functional assays, especially in settings of ART suppression in which T cells are less likely to have recently encountered antigen.

$CD8^+$ T cell recall cytotoxicity is associated with reduced HIV-1 reservoir size and activity
To investigate the potential impact of $CD8^+$ T cells capable of mounting highly cytolytic responses against autologous HIV-1 epitopes on persistent HIV-1 reservoirs during prolonged ART, we measured total and intact proviral DNA and unspliced cell-associated HIV-1 RNA across 49 participants with persistent virological suppression for at least one year prior to sampling. Participants with high $CD8^+$ T cell proliferation and recall cytotoxicity harbored lower total (mean 85.1 vs. 254.1 copies/10^6 PBMCs, Fig. 2E) and intact (mean 3.9 vs. 32.3 copies/10^6 PBMCs) proviral HIV-1 DNA (Figs. 2F, S4), and significantly lower cell-associated HIV-1 RNA (mean 130.2 vs. 751.3 copies/10^6 PBMCs, Fig. 2G) at the same sample time points used for immunologic assessments.

These associations may indicate a role for $CD8^+$ T cell recall cytotoxicity in limiting HIV-1 persistence, and/or the converse. To assess whether superior HIV-specific $CD8^+$ T cell functionality during prolonged ART may be associated with evidence of limited pre-ART disease progression, we analyzed demographic, clinical, and treatment variables. There were no significant associations between high cytolytic potential and measures of disease progression prior to ART, such as peak plasma viral load or nadir CD4 counts (Fig. S5, Table S1), suggesting that superior $CD8^+$ T cell functionality in this cohort is unlikely to be the result of superior pre-ART control of HIV-1. Instead, these results support a role for $CD8^+$ T cell recall cytotoxicity in limiting the size of transcriptionally active persistent HIV-1 reservoirs in PWH.

Peripheral immune responses to HIV-1 during analytical treatment interruption
To further evaluate the impact of immune cell function on HIV-1 persistence and post-treatment viral rebound, we studied the cellular immune response in one HEAL participant, H047, who consented to participate in an analytical treatment interruption (ATI) substudy. Plasma viral loads were measured weekly and PBMCs were obtained bi-weekly during ATI (Table S2).

Plasma viremia was detectable by two weeks post-ATI and reached a peak of 5.16 $\log_{10}$ HIV-1 RNA copies/ml at week 5 post-ATI, before spontaneous 3.9-fold reduction to 4.56 $\log_{10}$ copies/ml by week 6 post-ATI over a span of 6 days (Fig. 3A). Due to protocol-defined criteria, ART was restarted after collection of the week 6 post-ATI peripheral blood sample and virus re-suppressed to <20 copies/ml within two weeks (Fig. 3A, Table S2). HIV-1 cell-associated RNA (caRNA) levels increased during ATI, but not to levels commensurate with plasma viremia; these markers returned to pre-ATI levels 4 weeks after ART re-initiation and remained unchanged one year later (Fig. S6). Unspliced HIV-1 RNA was detected at higher levels than polyadenylated HIV-1 RNA during ART, consistent with prior literature (*27*), but their ratios reversed during detectable plasma viremia. One year after ATI, HIV-1 persistence markers were similar to pre-ATI levels.

To comprehensively assess the peripheral immune response to HIV-1 during and after ATI, we isolated PBMC from biweekly longitudinal samples, performed integrated single-cell multiomics, and assessed changes in T cell receptor (TCR) and B cell receptor (BCR) clonality, surface protein and gene expression. 37,462 PBMC across six time points were included in longitudinal CITE-seq and immune profiling analyses (Fig. 3B, Data file S2). While the frequencies of most cell types were stable during the treatment interruption, we observed a 1.7-1.9-fold expansion of NK cells that began in week 2 of ATI, remained elevated through week 6 of ATI, and then contracted to approximately half of pre-ATI levels after ART was restarted (Fig. 3C). This NK cell expansion was characterized by a cytolytic terminal effector phenotype (Fig. S7) (*28, 29*). A sub-clustering analysis of $CD8^+$ T cells demonstrated a 7-8-fold expansion of one subcluster (cluster 2) that began in week 4 of ATI after the NK expansion, was maintained through ART restart, and then contracted 4 weeks after ART re-initiation (Figs. 3D-E, S8A). Dynamic shifts in TCR clonotypes accompanied ATI (Fig. 3F). The most prevalent CD8 clonotype pre-ATI comprised 2.7% of all clonotypes (CSARLRTSGHDSTDTQYF). This and a sub-dominant clonotype (CASSVGQGSALGYTF) each expanded 2.7-2.9-fold during ATI and were enriched among cluster 2, whereas other minor clonotypes decreased up to 2.5-fold in frequency (Data file S2). A transient $CD8^+$ T cell population (cluster 8) was identified in the second week of treatment interruption when viremia was first detected (Fig. 3D-E). This cluster expressed TCRs matching cluster 2 (Data file S2) but was distinguished by a hypoxia-adapted, glycolysis-driven cellular program (Fig. S8B-F). Some B cell subsets also increased during ATI but without clonal expansion, while changes in $CD4^+$ T cell subpopulation proportions were not observed (Fig. S9). Together, these findings provide detailed kinetics of concurrent and sequential responses to HIV-1 recrudescence by different immune cell subsets.

$CD8^+$ T cell recall cytotoxicity coincides with partial suppression of rebound viremia

In parallel, we isolated HIV-1 epitope-specific $CD8^+$ T cells from H047 during ATI for CITE-seq and immune profiling. The immunodominant $CD8^+$ T cell response in this participant targeted the HLA-B*44-restricted Gag AEQASQEVKNW (AW11) epitope. Approximately 4.5% of total $CD8^+$ T cells targeted Gag AW11 at baseline and were highly proliferative (12% CFSE-low) and moderately cytolytic (52 AUC) *in vitro* (Fig. 4A). The rapid reduction in viral load observed at 6 weeks post-ATI, prior to ART reinitiation, was associated with concurrent *in vivo* expansion of Gag AW11-specific cells from 4.5% to 11.4% of total $CD8^+$ T cells, but not of subdominant HLA-B*18-restricted Nef YPLTFGWCF (YF9)-specific $CD8^+$ T cells (Fig. 4B). This *in vivo* expansion of AW11-specific cells (2.5-fold) was remarkably similar in magnitude to

the response of these cells to *in vitro* peptide stimulation (2.7-fold; Fig. 4A), further supporting the predictive value of *in vitro* proliferation assays. One year following ATI, the AW11-specific $CD8^+$ T cell response retained comparable *ex vivo* frequency, *in vitro* proliferative capacity and recall cytotoxicity to pre-ATI (Fig. 4C), suggesting that ATI did not have a detrimental impact on the quality of HIV-specific $CD8^+$ T cell functionality in this participant.

To further evaluate the $CD8^+$ T cell response to HIV-1 recrudescence at epitope-specific and temporal resolution, a total of 7,500 HIV-1 Gag AW11-specific $CD8^+$ T cells were grouped into six clusters based on differential gene expression (Fig. 4D), of which cluster 0 predominated at early time points (Fig. 4E,F). After re-emergence of viremia, the frequency of cells in cluster 0 decreased and a majority of HIV-specific $CD8^+$ T cells were instead found in cluster 1 (Fig. 4E,F). This change was associated with an increase in expression of genes and surface proteins associated with T cell activation and cytotoxic effector differentiation (Fig. 4G-I, Data file S3), including CD38, HLA-DR, *PRF1*, and *GZMB*; and a concomitant decrease in T cell quiescence as indicated by *IL7R*/CD127 (Fig. 4J-N). Most HIV-specific cells remained in this differentiated state for at least four weeks following reinitiation of ART as viremia declined (Fig. 4F).

To validate these findings by orthogonal methods, we also assayed longitudinal H047 ATI samples by flow cytometry and assessed *in vivo* HIV-specific $CD8^+$ T cell activation as measured by CD38 and HLA-DR co-expression, proliferation as measured by Ki-67 staining, and secondary cytotoxic effector differentiation as measured by perforin and granzyme B co-expression among pHLA $multimer^+$ cells. Rapid reduction of plasma viral load was accompanied by pronounced increases in activation, proliferation, and cytotoxicity of HIV-specific $CD8^+$ T cells (Fig. 4O). Together, these results indicate that functional HIV-1 epitope-specific $CD8^+$ T cells in H047 may contribute to attenuation of rebound viremia.

$CD8^+$ T cell clonotypes with distinct phenotypes expand in parallel during ATI

Clonotypic analysis based on TCRβ CDR3 sequences revealed that the Gag AW11-specific response in H047 was oligoclonal, with more than 75% of cells belonging to a single clonotype (Fig. 5A). AW11-specific clonotypes represented the 8 most abundant TCRs among total $CD8^+$ T cells identified in our single-cell PBMC analysis, including those in $CD8^+$ T cell subclusters 2 and 8 that responded to rebound viremia (Fig. 3F, Data file S2), further validating our epitope mapping approach. As the AW11-specific $CD8^+$ T cell population expanded in response to HIV-1 rebound (Fig. 4B), its clonotypic composition was largely maintained, except for one minor clonotype (CASSLYSNQPQHF) that expanded from less than one percent to greater than four percent of the response (Fig. 5B). Clonotypes differed significantly in gene and surface expression at baseline (Fig. 5C,D), with the dominant clonotype comprising clusters 0, 1, 3, and 5, and subdominant clonotypes comprising clusters 2 and 4 (Fig. 5A).

Prior to rebound viremia, the dominant clonotype expressed exhausted T cell gene and surface signatures marked by elevated PD-1, TIGIT, and *TOX* whereas the largest subdominant clonotype was more quiescent with elevated expression of CD226 and *TCF7* (Fig. 5E-I). Despite their phenotypic differences, both clonotypes expanded similarly by 2.7-2.9 fold *in vivo* during ATI (Data file S2), maintained their relative frequencies within AW11-specific $CD8^+$ T cells during their expansion in response to recrudescent viremia (Figs. 5B, 4B), and demonstrated comparable increases in activation and cytotoxic effector differentiation (Fig. 4D-E,J-N).

Notably, the *TCF7*$^+$ *TOX*$^+$ PD-1$^+$ CD8$^+$ T cells that comprised the dominant clonotype at baseline (cluster 0) resembled stem-like (also known as progenitor-exhausted) cells. Stem-like cells have been shown by multiple groups to be important for control of chronic viral infections and for memory formation upon removal of persistent antigen (*30-34*), which may also occur during ART-mediated HIV-1 suppression. The lack of an observed expansion disadvantage of this stem-like clonotype 1 relative to the more quiescent and less exhausted clonotype 2 indicates their comparable functionality *in vivo*, consistent with our *in vitro* phenotyping results (Fig. S3). Our results suggest that both stem-like and quiescent memory CD8$^+$ T cells with strong proliferative and cytolytic capacities may limit viral persistence during ART and recrudescence during ATI in a subset of PWH treated during chronic infection.

DISCUSSION

In this study we investigated the functionality of CD8$^+$ T cell responses against autologous HIV-1 epitopes during prolonged ART and their association with viral persistence markers. We observed unexpectedly high HIV-specific recall cytotoxicity in 17% of PWH who initiated ART during chronic progressive infection. These individuals harbored smaller and less transcriptionally active persistent viral reservoirs, relative to individuals with poor HIV-specific recall cytotoxicity. We also observed *in vivo* expansion and recall cytotoxicity of HIV-1 epitope-specific memory CD8$^+$ T cells concurrently with diminished rebound viremia in a participant who underwent ATI. We thoroughly characterized this epitope-specific CD8$^+$ T cell response to recrudescent viremia at temporal, clonotypic, and single-cell resolution, revealing that clonotypes with progenitor-exhausted and quiescent memory-like features expand comparably during attenuated viremia following ATI. These results suggest a potential role for CD8$^+$ T cell functionality in limiting HIV-1 reservoir persistence during therapy and rebound viremia following ART interruption, offering valuable guidance for the development of immunotherapeutic approaches to combat HIV-1 persistence.

Our results highlight the importance of evaluating CD8$^+$ T cell function at epitope-specific resolution and following re-exposure to autologous cognate antigen. While there is robust evidence that CD8$^+$ T cells from spontaneous HIV-1 controllers harbor stem-like proliferative capacity and recall cytotoxic potential against non-escaped epitopes [reviewed in (*1*)], their roles in limiting HIV-1 persistence during ART and rebound viremia during ATI in noncontrollers are less clear. Although persistent HIV-1 reservoirs are largely sensitive to recognition by circulating T cells (*35, 36*), individuals who fail to spontaneously control HIV-1 typically harbor dysfunctional virus-specific CD8$^+$ T cells associated with elevated expression of exhaustion-associated inhibitory receptors, such as PD-1 (*37*). Suppressive ART reduces inhibitory receptor expression but typically fails to restore HIV-specific CD8$^+$ T cell functionality as measured by proliferation and elimination assays (*8*). Consistent with this, we observed similar levels of PD-1 expression on functional and dysfunctional HIV-specific CD8$^+$ T cells *ex vivo* during prolonged ART and similar *in vivo* expansion of PD-1^{high} and PD-1^{low} HIV-specific CD8$^+$ T cells during ATI, further establishing a disconnect between inhibitory receptor expression and CD8$^+$ T cell functionality. This disconnect underscores the importance of measuring the functional potential of responses following antigen re-exposure rather than indirect *ex vivo* markers of functionality, especially in settings in which prolonged ART-mediated suppression of HIV-1 limits *in vivo* antigen exposure. Moreover, mutational escape from CD8$^+$ T cell recognition can result in retention of functionality through viral evasion of chronic stimulation (*38*). Thus, evaluation of

autologous epitope targeting provides necessary context for interpreting relevant functionality. Five of the sixteen proliferative responses we identified did not recognize autologous epitopes, and another eight recognized autologous epitopes that differed from HIV-1 consensus sequences. Absent evaluation of autologous cross-recognition, the five escaped responses would likely be incorrectly interpreted as functional, and half of the functional responses would likely be interpreted as escaped. For these reasons, functionality assessments in response to stimulation by consensus viral peptide pools or cells infected by laboratory virus strains may also be inaccurate.

Although ART does not typically restore HIV-specific $CD8^+$ T cell functionality, prolonged ART has in some cases been associated with superior $CD8^+$ T cell responses (*20, 39*), especially if initiated early during acute infection to limit the onset of T cell dysfunction (*9, 10*). Early ART initiation has also been associated with smaller HIV-1 reservoirs (*11-15, 40, 41*) and improved control of rebound viremia upon ATI (*16-19, 42*). Repeated ART interruption can also boost $CD8^+$ T cell immunity, which was associated with transient control of viremia in PWH treated during early but not during chronic infection (*43-45*). Importantly, neither treatment lapses, earlier ART initiation, prior spontaneous control nor limited disease progression were evident among the 17% of participants with high HIV-specific recall cytotoxicity. Although it was not possible in our study to access longitudinal samples from before ART to distinguish retention from improvement of $CD8^+$ T cell functionality, a recent study from an independent cohort of PWH reported functional rejuvenation following long-term ART that was associated with clonal succession (*20*). Despite its *in vitro* and *in vivo* functionality, the dominant clonotype functionally responding to treatment interruption in our study exhibited *ex vivo* signatures of chronic antigen stimulation, which may be inconsistent with recent clonal succession. Further research is warranted to identify precise mechanisms by which $CD8^+$ T cell functionality can be maintained or restored in PWH and to develop interventions to obviate the need for lifelong ART.

The impact of HIV-specific $CD8^+$ T cell functionality on HIV-1 persistence during prolonged ART initiated during chronic infection is not well understood. Prior studies have inferred immune selection of reservoirs by HIV-1 sequencing analysis (*46-49*) but have not demonstrated direct associations with immune cell functionality. In our study, participants with high recall cytotoxicity against autologous HIV-1 epitopes harbored smaller and less transcriptionally active reservoirs. It is plausible that this association could represent effects of functional $CD8^+$ T cells on HIV-1 persistence, the converse, or both. We did not have access to sufficient longitudinal specimens to compare reservoir decay rates in the presence or absence of functional $CD8^+$ T cell responses against autologous proviral epitopes, which will be important to evaluate in future studies. While it is challenging to infer directionality from associations, participants with highly functional HIV-specific $CD8^+$ T cells during prolonged ART did not exhibit clinical measures of reduced disease progression or immune activation/exhaustion. It is noteworthy that the association was strongest between $CD8^+$ T cell functionality and the size of the transcriptionally active portion of the reservoir during ART, and weakest for the size of the intact portion of the reservoir, because while viral transcription is a prerequisite for antigen presentation to $CD8^+$ T cells, intactness is not (*50*), further suggesting an impact of functional $CD8^+$ T cells on HIV-1 persistence during ART. While participants with superior HIV-specific $CD8^+$ T cell functionality had smaller reservoirs, several participants with poor functionality also harbored small reservoirs, suggesting that $CD8^+$ T cell functionality is not required for but may contribute to

limited HIV-1 persistence. Thus, future evaluation of complementary mechanisms by which HIV-1 persistence can be limited may also be informative.

Immune control of HIV-1 following ART interruption is a multifaceted process that remains to be fully elucidated. Prior studies have implicated several contributing factors, including polyfunctional HIV-specific $CD4^+$ T cells (*51*), autologous neutralizing humoral immune responses (*52, 53*), NK cell and Gag-specific $CD8^+$ T cell responses (*53, 54*). As memory $CD8^+$ T cells generally lack constitutive cytotoxicity without recent antigen exposure, they are unlikely to prevent HIV-1 rebound and are generally not associated with time to onset of viral rebound, which itself is not well correlated with set-point plasma viral load (*55, 56*). However, $CD8^+$ T cell recall cytotoxicity may play important roles in limiting, suppressing, or controlling recrudescent viremia. Due to clinical concerns, most ATI studies re-initiate ART before the ability of secondary effector cell responses to control rebound viremia can be ascertained (*57*). Although limited to a single participant, our study was no exception; ART restart criteria were met before set-point viremia was reached. Our assessments of HIV-1 persistence markers during ATI suggest, anecdotally, that large increases in plasma viremia can be generated initially without correspondingly large increases in intracellular HIV-1 RNA species. Understanding these virus dynamics in more detail may inform the evaluation of investigational HIV-1 latency reversal agents. HIV-1 recrudescence was accompanied by early expansion of effector NK cells and a transient increase in glycolytic signatures among HIV-1-epitope-specific $CD8^+$ T cells. Prior to ART resumption, rapid partial suppression of viremia was evident and was accompanied by *in vivo* proliferation and cytotoxic effector differentiation of HIV-1 epitope-specific $CD8^+$ T cells, consistent with an impact of recall cytotoxicity on viremia.

Investigational infusion of broadly neutralizing antibodies at the time of ATI has been shown to durably prevent or control rebound viremia in some cases, and this effect has also been associated with $CD8^+$ T cell responses (*58-65*), providing unique opportunities to define cellular immune determinants of post-treatment control with reduced safety risk. Emerging evidence further suggests that proliferation of HIV-specific $CD8^+$ T cells is associated with post-intervention control of viremia following combination immunotherapy (*21-23*). Interestingly, the frequency of highly functional responses we observed among PWH during prolonged ART (17%) is similar to the frequency of post-intervention control observed following infusion of broadly neutralizing anti-HIV-1 antibodies (*59, 60*), consistent with a potential role for $CD8^+$ T cell functionality in this process. Collectively, these results highlight recall cytotoxicity of memory $CD8^+$ T cells targeting autologous HIV-1 as an important parameter in the development and evaluation of immunotherapeutic strategies to combat HIV-1 persistence.

MATERIALS AND METHODS

Study design

This non-interventional study was designed to assess the range of cytolytic activity among $CD8^+$ T cells targeting autologous HIV-1 epitopes during prolonged ART and its potential impact on virus persistence. Peripheral blood was collected from ART-suppressed PWH enrolled in the HIV Eradication and Latency (HEAL) cohort, a longitudinal study of PWH. The institutional review board at Brigham and Women's Hospital (Mass General Brigham Human Research Committee – MGB HRC) approved the study protocol. Written informed consent was obtained

from all participants. Experimenters were blinded to all clinical data. Cohort size (*n*= 60) was determined by specimen availability. Plasma HIV-1 viral loads, complete blood counts, and demographic information were extracted from electronic medical records with participant consent. All participants were treated with suppressive ART for a minimum of one year (median 19 years, IQR 11-22 years) prior to sample collection. PBMCs were isolated by density gradient centrifugation and cryopreserved. PBMCs from a separate group of spontaneous HIV-1 controllers who maintained plasma viral loads below 2,000 HIV-1 RNA copies/ml for several years without ART from the Ragon Institute cohort were included for comparison to HEAL participants across immunologic assays following MGB HRC secondary use approval.

Participant H047 enrolled in an elective, IRB-approved HEAL ATI sub-study after meeting stringent enrollment criteria derived from consensus recommendations for ATI studies (*57*), risk counseling, and written informed consent. Peripheral blood was collected bi-weekly and plasma viral load was monitored weekly during ATI. Pre-determined ART restart criteria included request by the participant or their HIV-1 healthcare provider, pregnancy, symptomatic HIV-1 disease, confirmed absolute CD4 value <350 cells/µl or CD4% less than 15, plasma viral load greater than or equal to 1,000 HIV-1 RNA copies/ml for 4 weeks or greater than 100,000 copies/ml at any time. After ART reinitiation, plasma viral loads and CD4 counts were monitored to ensure full virus re-suppression was achieved.

HLA genotyping

Frozen dry cell pellets were sent to the American Red Cross Histocompatibility Laboratory Services (Dedham, Mass.) for high-resolution genotyping of the *HLA-A, -B,* and *-C* loci. *HLA-B* alleles associated with low or high plasma viral loads in a genome-wide association study of natural HIV-1 infection (*25*) were considered as protective (*HLA-B*14, B*27, B*52, B*57*) or risk (*HLA-B*07, B*08, B*35*), respectively, while all other *HLA*-B alleles were considered neutral. Allele frequencies were compared to the United States population (*24*) and to 10 spontaneous HIV-1 controllers who were genotyped previously by the Carrington laboratory at the United States National Cancer Institute.

HIV-1 epitope-specific response mapping by IFN-γ elispot

Frozen PBMCs were thawed at 37°C, recovered in RPMI media (Sigma-Aldrich) supplemented with 10% fetal bovine serum (FBS, Sigma; R10) overnight, resuspended at $1x10^6$/mL in R10, and plated 200 µL per well in Immobilon-P 96-well microtiter plates (Millipore) pre-coated with 2 µg/mL anti-IFN-γ (clone DK1, Mabtech). Individual HLA-optimal HIV-1 peptides matched to each subject's *HLA* genotype, as listed previously (*3*), were added at 1 µM and incubated at 37°C overnight. Triplicate negative control wells did not receive peptide and positive control wells were treated with 1 µg/ml anti-CD3 (clone OKT3, Biolegend) and 1 µg/ml anti-CD28 (clone CD28.8, Biolegend) antibodies. ELISPOT assay was performed using manufacturer's protocol with anti-IFN-γ (clone 1-DK1, Mabtech) capture, biotinylated anti-IFN-γ (clone B6-1, Mabtech) detection, Streptavidin-ALP (Mabtech) and AP Conjugated Substrate (BioRad) followed by disinfection with 0.05% Tween-20 (Thermo Fisher) and analysis using S6 Macro Analyzer (CTL Analyzers). Responses greater than 10 spots per well (50 spots per 10^6 PBMCs) and 3-fold above negative controls were scored as positive. Of 66 participants screened, 6 (9%) were excluded from downstream analyses due to low cell viability and/or high nonspecific background in elispot, which precluded interpretation of results.

Proliferation assay
Proliferation was measured by CFSE dilution as described previously (*3*). Briefly, frozen PBMCs were thawed at 37°C, recovered in RPMI media (Sigma-Aldrich) supplemented with 10% fetal bovine serum (FBS, Sigma; R10) overnight, then stained at 37°C for 20 minutes with 0.5 µM CellTrace CFSE (Thermo Fisher) as per manufacturer's protocol. Cells were then quenched and washed twice with R10 media, resuspended at $1x10^6$/mL in R10, and plated at 200 µL per well in 96-well round-bottom polystyrene plates (Corning). Individual HLA-optimal HIV-1 peptides matched to each subject's *HLA* genotype, as listed previously (*3*), were added at 1 µM and incubated at 37°C for 6 days before flow cytometric assessment. Triplicate negative control wells did not receive peptide and positive control wells received 1 µg/ml anti-CD3 (clone OKT3, Biolegend) and 1 µg/ml anti-CD28 (clone CD28.8, Biolegend) antibodies. On day 6, cells were stained using Live/Dead Violet viability dye (Thermo Fisher), AlexaFluor700-anti-CD3 (clone SK7, Biolegend), and APC-anti-CD8 (clone RPA-T8, Biolegend), then analyzed by flow cytometry. Responses above 5% CFSE-low, equivalent to the mean proliferation of HIV-specific $CD8^+$ T cell responses in spontaneous controllers, were considered to have high proliferative capacity and were subsequently validated in triplicate; reported values represent averages of triplicates.

HIV-1 proviral epitope sequencing
Genomic DNA was extracted from $CD4^+$ T cells isolated from 20 million PBMCs per sample using the EasySep $CD4^+$ T cell isolation kit (StemCell Technologies) followed by the QIAamp DNA Blood Mini kit (Qiagen) via the manufacturer's protocols. PCR amplification of HIV-1 proviral DNA was performed using nested-PCR primers specific for *gag*, *pol*, and/or 3' half amplicons, as described previously (*66*). Technical replicates for each PCR amplicon of correct size were gel-purified (Qiagen) and pooled for sequencing. Sequencing via Illumina MiSeq, assembly, and alignment to HXB2 reference were performed by the Mass General Brigham Center for Computational & Integrative Biology DNA Core (Boston, Mass) for amplicons containing epitopes targeted by HIV-specific $CD8^+$ T cell responses of interest as determined by functional response mapping experiments. In cases where multiple autologous epitope variants were detected, all were tested for cross-recognition.

Variant peptide cross-recognition assay
HIV-1 epitope-specific responses for which epitope variants were identified among autologous provirus were tested for cross-recognition of or mutational escape from $CD8^+$ T cell recognition. PBMCs were stimulated for 4 hours with 1 µM of HLA-optimal peptides of clade B HIV-1 consensus and each autologous sequence observed in provirus. BV711-conjugated anti-CD107A (clone H4A3, Biolegend) was included during stimulation to measure degranulation. GolgiStop and GolgiPlug (BD Biosciences) were added 2 hours post-stimulation to enable intracellular cytokine staining. Cells were stained with Live/Dead Violet, BV605-conjugated anti-CD3 (clone SK7, Biolegend) and BUV395-conjugated anti-CD8 (clone RPA-T8, BD Biosciences), fixed and permeabilized using Cytofix/Cytoperm (BD Biosciences), stained for intracellular PE-Cy7-conjugated anti-IFN-γ (clone B27, Biolegend) and analyzed via flow cytometry. Recognition was considered maintained if the frequency of $CD107A^+$ IFN-γ^+ $CD8^+$ T cells upon autologous variant peptide stimulation was greater than 50% for all observed variants or escaped if less than 50% that of clade B consensus peptide stimulation for any observed variant.

Phenotypic cytometry
Peptide-HLA monomers for responses of interest were purchased from ImmunAware (Copenhagen, Denmark). Tetramers were produced by multimerization with APC-conjugated streptavidin (Biolegend) as per manufacturer's protocol and stored at 4°C for a maximum of 24 weeks prior to use. Staining was performed using 4 nM individual APC-conjugated pHLA tetramers at 4°C for 30 minutes after 30-minute pre-treatment with 50 nM dasatinib to prevent *in vitro* cell activation and activation-induced cell death for phenotypic analysis. Cells were then stained with Live/Dead Near-IR viability dye (Thermo Fisher), BV510-conjugated anti-CD3 (clone SK7, Biolegend), BUV805-anti-CD8 (clone RPA-T8, BD Biosciences), BUV395-anti-CD45RA (clone HI100, BD Biosciences, RB780-anti-CD62L (clone DREG-56, BD Biosciences), BV711-anti-CD127 (clone A019D5, Biolegend), PE-Dazzle 594-anti-CD38 (clone HB7, Biolegend), and RB705-anti-PD-1 (clone EH12.1, BD Biosciences) for 30 minutes at 4°C before fixation and permeabilization with eBiosciences Foxp3/Transcrption Factor Staining kit (Thermo) as per manufacturer's protocol, intracellular staining for FITC-anti-granzyme B (clone GB11, Biolegend), and intranuclear staining for PE-anti-TCF1 (clone C63D9, Cell Signaling Technology). Cells were analyzed by flow cytometry. Samples with viability below 50% or fewer than 50 live HIV-specific pHLA-tetramer$^+$ CD8$^+$ T cells were excluded from downstream analyses.

Expanded antigen-specific elimination assay
Recall cytotoxicity of HIV-1 epitope-specific memory CD8$^+$ T cell responses was measured using the expanded antigen-specific elimination assay (EASEA) as per our published protocol (*26*), for all proliferative responses (>5% CFSE-low) and a representative sampling of nonproliferative responses that were immunodominant based on IFN-γ elispot. Rather than per-cell cytotoxicity, this assay measures per-response endpoint cytotoxicity following *in vitro* recall. Briefly, PBMCs were rested overnight in R10 then incubated with 100 ng/ml individual HLA-optimal HIV-1 peptide for six days to expand antigen-specific effector cells. Target CD4$^+$ T cells were isolated from PBMC by negative magnetic separation (StemCell Technologies), activated in 24-well non-treated polystyrene plates (Corning) pre-coated with 2 mg/ml anti-CD3 (clone OKT3, Biolegend) at 1-2 million cells/ml in R10 with 2 mg/ml anti-CD28 (clone CD28.2, Biolegend) and 50 U/ml IL-2 (Peprotech) at 37 C overnight, then expanded in treated 24-well plates (Corning) at 2 million cells/ml in R10 with 50 U/mL IL-2 at 37 C for five days. 50% of target cells were pulsed for 30 minutes at 37 C with 1 μM peptide and labeled with CellTrace Far Red dye (Thermo Fisher) and mixed with unpulsed target cells 1:1, then labeled with CellTrace Violet dye (Thermo Fisher). After six days of expansion, CFSE-labeled effector CD8+ T cells were isolated from pooled mononuclear cells by negative magnetic separation (StemCell Technologies) and co-cultured with target cells at effector:target (E:T) ratios of 0:1, 1:1, 2:1, 4:1, and 8:1 with 50,000 target cells/well in a treated 96-well polystyrene plate (Corning) for 4 hours. Effector-only populations were stained with APC-conjugated pHLA tetramers and all samples were stained with BV605-conjugated anti-CD3 (clone SK7, Biolegend), BUV395-conjugated anti-CD8 (clone RPA-T8, BD Biosciences), BV711-conjugated anti-CD4 (clone RPA-T4, Biolegend) and Live/Dead Near-IR (Thermo Fisher) then analyzed by flow cytometry. Results were gated as described previously and percent elimination and AUC were calculated as described previously (*3, 26*). Responses above 100 AUC, equivalent to the first-quartile recall

cytotoxicity of immunodominant HIV-specific $CD8^+$ T cell responses from spontaneous controllers, were considered to have high recall cytotoxicity.

Infected cell elimination assay

The assay described above was adapted to measure elimination of infected cells by proliferative HIV-1 Gag-specific responses from HEAL participants and spontaneous controllers via the following protocol modifications. PBMCs were labeled with CellTrace Violet dye (Thermp Fisher) instead of CFSE to avoid interference with GFP. $CD4^+$ T cells were infected with VSV-G-pseudotyped $HIV_{NL4-3\Delta Env-EGFP}$ (NIH AIDS Reagent Program, Division of AIDS, NIAID, NIH, Cat#11100 (*67*)) for the final 3 days of culture. Prior to coculture with autologous $CD8^+$ T cells, productively infected cells with downmodulated CD4 were enriched by magnetic CD4 depletion (EasySep CD4 Positive Selection Kit, StemCell Technologies) and mixed with autologous uninfected CD4 T cells to a final infection rate ~30%, then labeled with CellTrace FarRed. Cocultures were incubated for 16 hours to enable sufficient sensitivity. Cells from PWOH were stimulated with an A*02-restricted CMV NLVPMVATV and were included as negative controls to estimate assay sensitivity.

HIV-1 reservoir measurements

Genomic DNA and total RNA were isolated from approximately $5x10^6$ peripheral blood mononuclear cells (PBMC) or total $CD4^+$ T cells (AllPrep DNA/RNA kit, Qiagen). Total HIV-1 DNA and unspliced cell-associated RNA (usRNA) levels were quantified in triplicate by real-time PCR as previously described, modified to include Taqman Universal Mastermix (DNA) or Taqman Fast Virus 1-Step Mastermix (RNA) (*68*). HIV-1 quantifications used forward primer 5'-TACTGACGCTCTCGCACC-3', reverse primer 5'-TCTCGACGCAGGACTCG-3', and probe 5' FAM-CTCTCTCCTTCTAGCCTC-MGB 3' (ThermoFisher Scientific). DNA cycling conditions in a total reaction volume of 25µL were 95°C for 15 min followed by 40 cycles of 95°C for 15 sec and 60°C for 1 min. RNA cycling conditions in a total reaction volume of 20µL were 55°C for 15 min, 95°C for 20 sec, followed by 40 cycles of 95°C for 3 sec and 60°C for 30 sec. Approximately 500ng of genomic DNA were assessed per well. For polyadenylated HIV-1 mRNA quantifications, 10uL (approximately 1 million cell equivalents) of RNA were run in triplicate using primers and probe targeting the nef to poly-A region of HIV-1 mRNA as previously described (*69*). The limits of quantification for total HIV-1 DNA and unspliced caRNA were 1 and 3 copies per reaction, respectively. Limits of detection were calculated per timepoint and participant sample, considering the average number of copies detected across triplicate measurements. Cell input numbers were quantified by human genome equivalents of CCR5 DNA using forward primer 5'-ATGATTCCTGGGAGAGACGC-3', reverse primer 5'-AGCCAGGACGGTCACCTT-3', and probe 5' FAM-CTCTCTCCTTCTAGCCTC-MGB 3' (ThermoFisher Scientific) as described (*68*). To calculate copies of HIV-1 caRNA per million cells, copy numbers were averaged and cell counts normalized to a CCR5 DNA reference. Our HIV-1 unspliced and poly(A) caRNA amplifications are both one-step qPCR assays that use an HIV-specific primer to synthesize cDNA. For poly(A) HIV-1 mRNA quantifications, copies per million cell equivalents were calculated by initial cell count prior to reactivation. Both HIV-1 usRNA and polyA assays used Taqman Fast Virus 1-Step Mastermix in a total reaction volume of 20µL and identical cycling conditions.

HIV-1 DNA from isolated PBMC DNA was measured using the cross-subtype intact proviral DNA assay (CS-IPDA) as described (*70, 71*), with minor modifications. Two multiplexed droplet digital PCR assays (Bio-Rad QX200) were performed per sample targeting conserved HIV-1 sequences and, to normalize data, a cell reference gene. Master mixes were prepared using 2X ddPCR Supermix for probes. The three primer/probe sets of cross subtype primers used in this study, which have been shown to bind to target regions of Subtype B, A, C, D (*70*), CS-IPDA 5'pol (Forward: 5'-WCCYTTARYTTCCCTCARATCACTCT-3'; Reverse: 5'-TACTGTATCATCTGCTCCTGTRTCTAAKAGAGCYTC-3'; Probe: 5'- TTGGCARCGACC-3' FAM, BHQ); CS-IPDA LTR/Gag (Forward: 5'-GACTAGCGGAGGCTAGAAGGAGAGA-3'; Reverse: 5'-CTAATTTTCCSCCDCTTAATAYTGACG-3'; Probe: 5'- ATGGGTGCGAGA-3' HEX, BHQ); and CS-IPDA Env (Forward: 5'-TVTTCMTTGGGTTCTTRGGAGCAGCAGG-3'; Reverse: 5'-GCACTATRCCAGACAATAVYTGTCTGGCCTGTACC-3'; Probe: 5'- AGCACKATGGG-3'; HEX, BHQ). To estimate the number of cells per reaction and correct for sheared DNA, separate reactions targeting two regions of the *RPP30* gene, RPP30-1 (Forward: 5'-GATTTGGACCTGCGAGCG-3'; Reverse: 5'-GCGGCTGTCTCCACAAGT-3'; Probe: 5'-CTGACCTGAAGGCTCT-3', HEX, MGB) and RPP30-2 (Forward: 5'-GACACAATGTTTGGTACATGGTTAA-3'; Reverse: 5'-CTTTGCTTTGTATGTTGGCAGAAA-3'; Probe: 5'-CCATCTCACCAATCATTCTCCTTCCTTC -3', FAM). Droplets were generated and subjected to PCR cycle: 95°C for 10 minutes, followed by 60 cycles of 94°C for 30 seconds, 59°C for 1 minute, and ending with 98°C for 10 minutes before holding at 4°C. To increase the assay sensitivity, we run CS-IPDA in multiple wells with the DNA from minimum of cell 500,000 cells. Data from replicate wells were summed and analyzed using QuantaSoft Data Analysis Software. Droplets containing a triple positive signal (*pol*+/*gag*+/*env*+) were considered intact, and all other droplets were considered defective with deletions. Relative DNA shearing was calculated using the ratio of single positive RPP30 droplets compared to the double positive population and was used to estimate the number of intact proviruses. The number of diploid cells in each reaction was determined by dividing the copies of RPP30 in half and correcting for the dilution factor for the HIV-1 reaction. Intact, defective, and total HIV-1 DNA were normalized to the number of cells and reported as copies/million PBMC. 11 participants with detectable plasma viral loads within one year of sampling were excluded from reservoir analyses.

Whole-PBMC single-cell multiomics

Cryopreserved PBMCs from longitudinal samples collected during ATI from participant H047 were thawed and rested overnight at 37°C in media that contained raltegravir 2 μM and tenofovir 2 μM (Selleckchem). Cells were then washed with Cell Staining Buffer (BioLegend) and incubated with Fc receptor blocking solution (Human TruStain FcX, Biolegend) for 10 minutes at 4ºC. Cells from individual time points were barcoded by unique hashtag oligonucleotide (HTO) antibodies (Biolegend) for 20–30 min at 4 °C and incubated with Sytox Blue Dead Cell Stain (Invitrogen) at room temperature for 15 min before live cell sorting (SONY SH800, Ragon Institute). Sorted live cells were subsequently incubated with TotalSeq-C Human Universal Cocktail V2.0 (BioLegend) for 30 min at 4 °C and washed three times with Cell Staining Buffer. Stained and barcoded cells were immediately loaded onto Chromium X instrument (10X Genomics) for library construction for T and B cell receptor variable-diversity-joining (V(D)J) diversity analysis, 5' gene expression and cell surface protein profiling.

Sequencing data for gene expression, antibody capture, and BCR/TCR V(D)J were processed using the Cell Ranger multi pipeline (10X Genomics, v 9.0.0) with the GRCh38 human reference genome, TotalSeq-C feature reference sequences, and human V(D)J reference sequences, respectively. Demultiplexed data from each sample were imported into R (v 4.4.0) and combined for joint analysis using Seurat (v 5.2.1). A total of 37,739 PBMC before filtering and 37,462 PBMC after filtering were obtained for subsequent analyses. RNA filtering criteria were: 1) number of UMIs (nCount_RNA) > 1500, 2) number of detected genes (nFeature_RNA) > 1000, 3) mitochondrial percentages (percent_mito) < 20, and 4) novelty (novelty) > 0.8. ADT filtering criteria were number of UMIs (nCount_ADT) > 400 and number of detected proteins (nFeature_ADT) > 100.

RNA data were normalized using SCTransform (*72*), and TCR V(D)J genes were excluded from the set of highly variable features prior to principal component analysis (PCA). A uniform manifold approximation and projection (UMAP) embedding was generated using the top 30 principal components. The antibody-derived tag (ADT) counts were normalized by centered log ratio (CLR) transformation, followed by PCA and UMAP. RNA and ADT modalities were then integrated using a weighted nearest neighbor (WNN) algorithm (*73*), and UMAP and clustering was computed on the WNN graph.

TCR and BCR data were imported into R and incorporated into the Seurat object using scRepertorie (*74*). TCR clonotypes were defined by the CDR3 amino acid sequence of the beta chain, and BCR clonotypes were defined using scRepertorie's strict definition, which is based on the normalized Levenshtein edit distance of CDR3 nucleotide sequences and V-gene usage. Clonal proportions were calculated as the relative abundance of each clonotype within the total immune repertoire of the sample.

Cell types were assigned using a reference-mapping approach with the Azimuth PBMC reference. $CD8^+$ T cells, $CD4^+$ T cells, B cells, and Natural Killer (NK) cells were subsequently subsetted and reanalyzed. Differentially expressed genes (DEGs) were identified using the FindMarkers function in Seurat.

HIV-specific $CD8^+$ T cell single-cell multiomics

Cryopreserved H047 PBMC were thawed and rested overnight before negative-selection magnetic $CD8^+$ T cell isolation (StemCell Technologies), then stained with APC-conjugated HLA-B*44 AEQASQEVKNW tetramer, Total-Seq C Human Universal Cocktail (Biolegend), and six unique Total-Seq C hashing antibodies (Biolegend) corresponding to biweekly sample time points during the treatment interruption (TI) following reinitiation of ART (RA). 40,490 sorted cells were encapsulated in GEM-wells using a Chromium controller (10X Genomics). Gene expression (GEX), surface protein expression (antibody-derived tags, ADT), and TCR (VDJ) libraries were generated using the 10X Chromium NextGEM Single Cell 5' v2 Dual Index kit with feature barcoding technology (10X Genomics) following the manufacturer's instructions. Libraries were pooled at a 5:1:1 GEX:ADT:VDJ ratio and sequenced on a NextSeq 2000 instrument with a 100-cycle P3 kit (Illumina).

Base-calling was performed using bcl2fastq and initial data-processing was performed via the Cell Ranger multi pipeline (10X Genomics, v 7.0.0) using refdata-gex-GRCh38-2020-A as a transcriptome reference and refdata-cellranger-vdj-GRCh38-alts-ensembl-5.0.0 as a VDJ reference. Gene expression (GEX), antibody capture (ADT), and TCR (VDJ) libraries were specified in the multi analysis config file. Surface protein barcodes and hashtag barcodes corresponding to time points were designated as “Antibody Capture” in the feature-reference file. After processing by Cell Ranger, the count matrix in sample_filtered_feature_bc_matrix was analyzed using the Seurat R package. Hash-tag level timepoint sample demultiplexing was performed using the HTOdemux() function of Seurat, and cells were removed for which HTO_classification.global was not "Singlet", hence removing cells with multiple or no hashtags. 9,947 AW11-specific cells were recovered, of which 7,500 passed filtering, to include 493 in sample TI0, 1872 in TI2, 866 in TI4, 916 in TI6, 1625 in AR2, and 1728 in AR4. The GEX library yielded 45,823 median reads, 1,787 median genes, and 3,778 median UMIs per cell. The ADT library yielded 1,375 median ADT UMIs per cell. The VDJ library yielded 6,663 cells with productive V-J spanning pairs, and 3 and 17 median TRA and TRB UMIs per cell, respectively. To avoid clustering driven by clonotype-specific TCR gene expression, gene features for which the symbols matched the regular expression "^TR[ABDG][VJC]" were removed from the data set prior to clustering (*75*). Using the Seurat function FindVariableFeatures(), 4,000 variable genes were selected for dimensionality reduction and differential expression analysis. Counts were log normalized, scaled and centered prior to dimensionality reduction and clustering. Clustering was performed using SNN clustering via Seurat’s Seurat::FindNeighbors FindClusters() function with the argument resolution = 0.35. TCR clonotypes were assigned on the basis of raw_clonotype_id from the vdj_tfiltered_contig_annotations.csv file generated by Cell Ranger. Differential expression was performed using Seurat’s FindMarkers() function. Pathway analysis was performed using the tmodCERNOtest() from the tmod R package version 0.46.2(*76*) using a subset of MSigDB version v7.5.1 (*77*) that included the hallmark (H), gene ontology, reactome, and KEGG gene sets. Gene set network analysis was performed using the GSNA R package, version 0.1.4.9, as previously described (*3, 78*).

Flow cytometry

All flow cytometry data was acquired at the Ragon Institute flow cytometry core facility using BD Symphony, Fortessa, and LSR-II cytometers. Fluorescence spillover compensation was applied using FACSDiva software (BD Biosciences) after collection of single-stained cell- or bead-based compensation controls (Thermo Fisher). Data was analyzed using FlowJo v10.10. Gating thresholds were established using appropriate negative controls, including fluorescence-minus-one and biological negative controls. Gates were applied consistently across all intra- and inter-sample comparisons.

Statistical analyses

Statistical analyses were performed using GraphPad Prism and R (vers.4.4.0). Assuming a general non-Normal distribution of the data, non-parametric tests based on ranks were used to compare continuous measurements across groups (Wilcoxon rank-sum tests), as well as categorical variables (Fisher’s exact tests), where needed. For the same reason, Spearman’s correlation coefficients (with corresponding tests) were preferred to Pearson’s, to verify monotonicity between measurements.

List of Supplementary Materials

Figures S1 to S9

Tables S1 to S2

Data files S1 to S3

References

1. D. R. Collins, G. D. Gaiha, B. D. Walker, CD8(+) T cells in HIV control, cure and prevention. *Nat Rev Immunol* **20**, 471-482 (2020).
2. M. R. Betts, M. C. Nason, S. M. West, S. C. De Rosa, S. A. Migueles, J. Abraham, M. M. Lederman, J. M. Benito, P. A. Goepfert, M. Connors, M. Roederer, R. A. Koup, HIV nonprogressors preferentially maintain highly functional HIV-specific CD8+ T cells. *Blood* **107**, 4781-4789 (2006).
3. D. R. Collins, J. M. Urbach, Z. J. Racenet, U. Arshad, K. A. Power, R. M. Newman, G. H. Mylvaganam, N. L. Ly, X. Lian, A. Rull, Y. Rassadkina, A. G. Yanez, M. J. Peluso, S. G. Deeks, F. Vidal, M. Lichterfeld, X. G. Yu, G. D. Gaiha, T. M. Allen, B. D. Walker, Functional impairment of HIV-specific CD8(+) T cells precedes aborted spontaneous control of viremia. *Immunity* **54**, 2372-2384 e2377 (2021).
4. G. D. Gaiha, E. J. Rossin, J. Urbach, C. Landeros, D. R. Collins, C. Nwonu, I. Muzhingi, M. N. Anahtar, O. M. Waring, A. Piechocka-Trocha, M. Waring, D. P. Worrall, M. S. Ghebremichael, R. M. Newman, K. A. Power, T. M. Allen, J. Chodosh, B. D. Walker, Structural topology defines protective CD8(+) T cell epitopes in the HIV proteome. *Science* **364**, 480-484 (2019).
5. H. Horton, I. Frank, R. Baydo, E. Jalbert, J. Penn, S. Wilson, J. P. McNevin, M. D. McSweyn, D. Lee, Y. Huang, S. C. De Rosa, M. J. McElrath, Preservation of T cell proliferation restricted by protective HLA alleles is critical for immune control of HIV-1 infection. *J Immunol* **177**, 7406-7415 (2006).
6. S. A. Migueles, A. C. Laborico, W. L. Shupert, M. S. Sabbaghian, R. Rabin, C. W. Hallahan, D. Van Baarle, S. Kostense, F. Miedema, M. McLaughlin, L. Ehler, J. Metcalf, S. Liu, M. Connors, HIV-specific CD8+ T cell proliferation is coupled to perforin expression and is maintained in nonprogressors. *Nat Immunol* **3**, 1061-1068 (2002).
7. S. A. Migueles, C. M. Osborne, C. Royce, A. A. Compton, R. P. Joshi, K. A. Weeks, J. E. Rood, A. M. Berkley, J. B. Sacha, N. A. Cogliano-Shutta, M. Lloyd, G. Roby, R. Kwan, M. McLaughlin, S. Stallings, C. Rehm, M. A. O'Shea, J. Mican, B. Z. Packard, A. Komoriya, S. Palmer, A. P. Wiegand, F. Maldarelli, J. M. Coffin, J. W. Mellors, C. W. Hallahan, D. A. Follman, M. Connors, Lytic granule loading of CD8+ T cells is required for HIV-infected cell elimination associated with immune control. *Immunity* **29**, 1009-1021 (2008).
8. S. A. Migueles, K. A. Weeks, E. Nou, A. M. Berkley, J. E. Rood, C. M. Osborne, C. W. Hallahan, N. A. Cogliano-Shutta, J. A. Metcalf, M. McLaughlin, R. Kwan, J. M. Mican, R. T. Davey, Jr., M. Connors, Defective human immunodeficiency virus-specific CD8+ T-cell polyfunctionality, proliferation, and cytotoxicity are not restored by antiretroviral therapy. *J Virol* **83**, 11876-11889 (2009).
9. Z. M. Ndhlovu, S. W. Kazer, T. Nkosi, F. Ogunshola, D. M. Muema, G. Anmole, S. A. Swann, A. Moodley, K. Dong, T. Reddy, M. A. Brockman, A. K. Shalek, T. Ndung'u, B. D. Walker, Augmentation of HIV-specific T cell function by immediate treatment of hyperacute HIV-1 infection. *Sci Transl Med* **11**, (2019).

10. H. Takata, J. C. Kakazu, J. L. Mitchell, E. Kroon, D. J. Colby, C. Sacdalan, H. Bai, P. K. Ehrenberg, A. Geretz, S. Buranapraditkun, S. Pinyakorn, J. Intasan, S. Tipsuk, D. Suttichom, P. Prueksakaew, T. Chalermchai, N. Chomchey, N. Phanuphak, M. de Souza, N. L. Michael, M. L. Robb, E. K. Haddad, T. A. Crowell, S. Vasan, V. G. Valcour, D. C. Douek, R. Thomas, M. Rolland, N. Chomont, J. Ananworanich, L. Trautmann, R. S. Rv254/Search, S. s. groups, Long-term antiretroviral therapy initiated in acute HIV infection prevents residual dysfunction of HIV-specific CD8(+) T cells. *EBioMedicine* **84**, 104253 (2022).
11. J. Ananworanich, N. Chomont, L. A. Eller, E. Kroon, S. Tovanabutra, M. Bose, M. Nau, J. L. K. Fletcher, S. Tipsuk, C. Vandergeeten, R. J. O'Connell, S. Pinyakorn, N. Michael, N. Phanuphak, M. L. Robb, Rv, R. S. s. groups, HIV DNA Set Point is Rapidly Established in Acute HIV Infection and Dramatically Reduced by Early ART. *EBioMedicine* **11**, 68-72 (2016).
12. M. J. Buzon, E. Martin-Gayo, F. Pereyra, Z. Ouyang, H. Sun, J. Z. Li, M. Piovoso, A. Shaw, J. Dalmau, N. Zangger, J. Martinez-Picado, R. Zurakowski, X. G. Yu, A. Telenti, B. D. Walker, E. S. Rosenberg, M. Lichterfeld, Long-term antiretroviral treatment initiated at primary HIV-1 infection affects the size, composition, and decay kinetics of the reservoir of HIV-1-infected CD4 T cells. *J Virol* **88**, 10056-10065 (2014).
13. M. Laanani, J. Ghosn, A. Essat, A. Melard, R. Seng, M. Gousset, H. Panjo, E. Mortier, P. M. Girard, C. Goujard, L. Meyer, C. Rouzioux, P. C. S. G. Agence Nationale de Recherche sur le Sida, Impact of the Timing of Initiation of Antiretroviral Therapy During Primary HIV-1 Infection on the Decay of Cell-Associated HIV-DNA. *Clin Infect Dis* **60**, 1715-1721 (2015).
14. L. Leyre, E. Kroon, C. Vandergeeten, C. Sacdalan, D. J. Colby, S. Buranapraditkun, A. Schuetz, N. Chomchey, M. de Souza, W. Bakeman, R. Fromentin, S. Pinyakorn, S. Akapirat, R. Trichavaroj, S. Chottanapund, S. Manasnayakorn, R. Rerknimitr, P. Wattanaboonyoungcharoen, J. H. Kim, S. Tovanabutra, T. W. Schacker, R. O'Connell, V. G. Valcour, P. Phanuphak, M. L. Robb, N. Michael, L. Trautmann, N. Phanuphak, J. Ananworanich, N. Chomont, R. V. S. S. s. g. Rv254/Search, Abundant HIV-infected cells in blood and tissues are rapidly cleared upon ART initiation during acute HIV infection. *Sci Transl Med* **12**, (2020).
15. M. C. Strain, S. J. Little, E. S. Daar, D. V. Havlir, H. F. Gunthard, R. Y. Lam, O. A. Daly, J. Nguyen, C. C. Ignacio, C. A. Spina, D. D. Richman, J. K. Wong, Effect of treatment, during primary infection, on establishment and clearance of cellular reservoirs of HIV-1. *J Infect Dis* **191**, 1410-1418 (2005).
16. C. Goujard, I. Girault, C. Rouzioux, C. Lecuroux, C. Deveau, M. L. Chaix, C. Jacomet, A. Talamali, J. F. Delfraissy, A. Venet, L. Meyer, M. Sinet, A. C. P. S. Group, HIV-1 control after transient antiretroviral treatment initiated in primary infection: role of patient characteristics and effect of therapy. *Antivir Ther* **17**, 1001-1009 (2012).
17. J. Z. Li, M. Melberg, A. Kittilson, M. Abdel-Mohsen, Y. Li, E. Aga, R. J. Bosch, E. R. Wonderlich, J. Kinslow, L. B. Giron, C. Di Germanio, M. Pilkinton, L. MacLaren, M. Keefer, L. Fox, L. Barr, E. Acosta, J. Ananworanich, R. Coombs, J. Mellors, S. Deeks, R. T. Gandhi, M. Busch, A. Landay, B. Macatangay, D. M. Smith, A. C. T. G. A. S. Team, Predictors of HIV rebound differ by timing of antiretroviral therapy initiation. *JCI Insight* **9**, (2024).
18. G. Namazi, J. M. Fajnzylber, E. Aga, R. J. Bosch, E. P. Acosta, R. Sharaf, W. Hartogensis, J. M. Jacobson, E. Connick, P. Volberding, D. Skiest, D. Margolis, M. C. Sneller, S. J. Little, S. Gianella, D. M. Smith, D. R. Kuritzkes, R. M. Gulick, J. W. Mellors, V. Mehraj, R. T. Gandhi, R. Mitsuyasu, R. T. Schooley, K. Henry, P. Tebas, S. G. Deeks, T. W. Chun, A. C. Collier, J. P. Routy, F. M. Hecht, B. D. Walker, J. Z. Li, The Control of HIV After Antiretroviral Medication Pause (CHAMP) Study: Posttreatment Controllers Identified From 14 Clinical Studies. *J Infect Dis* **218**, 1954-1963 (2018).
19. J. P. Williams, J. Hurst, W. Stohr, N. Robinson, H. Brown, M. Fisher, S. Kinloch, D. Cooper, M. Schechter, G. Tambussi, S. Fidler, M. Carrington, A. Babiker, J. Weber, K. K. Koelsch, A. D.

Kelleher, R. E. Phillips, J. Frater, S. P. Investigators, HIV-1 DNA predicts disease progression and post-treatment virological control. *Elife* **3**, e03821 (2014).

20. E. White, L. Papagno, A. Samri, K. Sugata, B. Hejblum, A. R. Henry, D. C. Rogan, S. Darko, P. Recordon-Pinson, Y. Dudoit, S. Llewellyn-Lacey, L. A. Chakrabarti, F. Buseyne, S. A. Migueles, D. A. Price, M. A. Andreola, Y. Satou, R. Thiebaut, C. Katlama, B. Autran, D. C. Douek, V. Appay, Clonal succession after prolonged antiretroviral therapy rejuvenates CD8(+) T cell responses against HIV-1. *Nat Immunol*, (2024).

21. M. J. Peluso, D. A. Sandel, A. N. Deitchman, S. J. Kim, T. Dalhuisen, H. P. Tummala, R. Tiburcio, L. Zemelko, G. M. Borgo, S. S. Singh, K. Schwartz, M. Deswal, M. C. Williams, R. Hoh, M. Shimoda, S. Narpala, L. Serebryannyy, M. Khalili, E. Vendrame, D. SenGupta, L. S. Whitmore, J. Tisoncik-Go, M. Gale, Jr., R. A. Koup, J. I. Mullins, B. K. Felber, G. N. Pavlakis, J. D. Reeves, C. J. Petropoulos, D. V. Glidden, M. H. Spitzer, L. Gama, M. Caskey, M. C. Nussenzweig, K. W. Chew, T. J. Henrich, S. A. Yukl, L. B. Cohn, S. G. Deeks, R. L. Rutishauser, Combination immunotherapy induces post-intervention control of HIV. *Res Sq*, (2025).

22. M. Altaf, T. Tipoe, C. Nel, H. Brown, N. Robinson, S. Collins, M. J. Lee, P. Zacharopoulou, L.-R. Cherrill, E. Falaschetti, M. Nussenzweig, M. Caskey, S. Fidler, J. Frater, Sustained T-Cell Mediated Immunity After LS-bNAbs in the RIO Trial: A Vaccinal Effect. *Topics in Antiviral Medicine* **33**, 506 (2025).

23. Z. Kiani, M. J. Olatotse, J. M. Urbach, M. Lichterfeld, J. D. Gunst, O. S. Sogaard, M. Caskey, M. Nussenzweig, B. D. Walker, D. R. Collins, HIV-Specific CD8+ T Cell Stemness Predicts Post-Intervention Control of Viremia. *Topics in Antiviral Medicine* **33**, 31-32 (2025).

24. M. Maiers, L. Gragert, W. Klitz, High-resolution HLA alleles and haplotypes in the United States population. *Hum Immunol* **68**, 779-788 (2007).

25. F. Pereyra, X. Jia, P. J. McLaren, A. Telenti, P. I. de Bakker, B. D. Walker, S. Ripke, C. J. Brumme, S. L. Pulit, M. Carrington, C. M. Kadie, J. M. Carlson, D. Heckerman, R. R. Graham, R. M. Plenge, S. G. Deeks, L. Gianniny, G. Crawford, J. Sullivan, E. Gonzalez, L. Davies, A. Camargo, J. M. Moore, N. Beattie, S. Gupta, A. Crenshaw, N. P. Burtt, C. Guiducci, N. Gupta, X. Gao, Y. Qi, Y. Yuki, A. Piechocka-Trocha, E. Cutrell, R. Rosenberg, K. L. Moss, P. Lemay, J. O'Leary, T. Schaefer, P. Verma, I. Toth, B. Block, B. Baker, A. Rothchild, J. Lian, J. Proudfoot, D. M. Alvino, S. Vine, M. M. Addo, T. M. Allen, M. Altfeld, M. R. Henn, S. Le Gall, H. Streeck, D. W. Haas, D. R. Kuritzkes, G. K. Robbins, R. W. Shafer, R. M. Gulick, C. M. Shikuma, R. Haubrich, S. Riddler, P. E. Sax, E. S. Daar, H. J. Ribaudo, B. Agan, S. Agarwal, R. L. Ahern, B. L. Allen, S. Altidor, E. L. Altschuler, S. Ambardar, K. Anastos, B. Anderson, V. Anderson, U. Andrady, D. Antoniskis, D. Bangsberg, D. Barbaro, W. Barrie, J. Bartczak, S. Barton, P. Basden, N. Basgoz, S. Bazner, N. C. Bellos, A. M. Benson, J. Berger, N. F. Bernard, A. M. Bernard, C. Birch, S. J. Bodner, R. K. Bolan, E. T. Boudreaux, M. Bradley, J. F. Braun, J. E. Brndjar, S. J. Brown, K. Brown, S. T. Brown, J. Burack, L. M. Bush, V. Cafaro, O. Campbell, J. Campbell, R. H. Carlson, J. K. Carmichael, K. K. Casey, C. Cavacuiti, G. Celestin, S. T. Chambers, N. Chez, L. M. Chirch, P. J. Cimoch, D. Cohen, L. E. Cohn, B. Conway, D. A. Cooper, B. Cornelson, D. T. Cox, M. V. Cristofano, G. Cuchural, Jr., J. L. Czartoski, J. M. Dahman, J. S. Daly, B. T. Davis, K. Davis, S. M. Davod, E. DeJesus, C. A. Dietz, E. Dunham, M. E. Dunn, T. B. Ellerin, J. J. Eron, J. J. Fangman, C. E. Farel, H. Ferlazzo, S. Fidler, A. Fleenor-Ford, R. Frankel, K. A. Freedberg, N. K. French, J. D. Fuchs, J. D. Fuller, J. Gaberman, J. E. Gallant, R. T. Gandhi, E. Garcia, D. Garmon, J. C. Gathe, Jr., C. R. Gaultier, W. Gebre, F. D. Gilman, I. Gilson, P. A. Goepfert, M. S. Gottlieb, C. Goulston, R. K. Groger, T. D. Gurley, S. Haber, R. Hardwicke, W. D. Hardy, P. R. Harrigan, T. N. Hawkins, S. Heath, F. M. Hecht, W. K. Henry, M. Hladek, R. P. Hoffman, J. M. Horton, R. K. Hsu, G. D. Huhn, P. Hunt, M. J. Hupert, M. L. Illeman, H. Jaeger, R. M. Jellinger, M. John, J. A. Johnson, K. L. Johnson, H. Johnson, K. Johnson, J. Joly, W. C. Jordan, C. A. Kauffman, H. Khanlou, R. K. Killian, A. Y. Kim, D. D. Kim, C. A. Kinder, J. T. Kirchner, L.

Kogelman, E. M. Kojic, P. T. Korthuis, W. Kurisu, D. S. Kwon, M. LaMar, H. Lampiris, M. Lanzafame, M. M. Lederman, D. M. Lee, J. M. Lee, M. J. Lee, E. T. Lee, J. Lemoine, J. A. Levy, J. M. Llibre, M. A. Liguori, S. J. Little, A. Y. Liu, A. J. Lopez, M. R. Loutfy, D. Loy, D. Y. Mohammed, A. Man, M. K. Mansour, V. C. Marconi, M. Markowitz, R. Marques, J. N. Martin, H. L. Martin, Jr., K. H. Mayer, M. J. McElrath, T. A. McGhee, B. H. McGovern, K. McGowan, D. McIntyre, G. X. McLeod, P. Menezes, G. Mesa, C. E. Metroka, D. Meyer-Olson, A. O. Miller, K. Montgomery, K. C. Mounzer, E. H. Nagami, I. Nagin, R. G. Nahass, M. O. Nelson, C. Nielsen, D. L. Norene, D. H. O'Connor, B. O. Ojikutu, J. Okulicz, O. O. Oladehin, E. C. Oldfield, 3rd, S. A. Olender, M. Ostrowski, W. F. Owen, Jr., E. Pae, J. Parsonnet, A. M. Pavlatos, A. M. Perlmutter, M. N. Pierce, J. M. Pincus, L. Pisani, L. J. Price, L. Proia, R. C. Prokesch, H. C. Pujet, M. Ramgopal, A. Rathod, M. Rausch, J. Ravishankar, F. S. Rhame, C. S. Richards, D. D. Richman, B. Rodes, M. Rodriguez, R. C. Rose, 3rd, E. S. Rosenberg, D. Rosenthal, P. E. Ross, D. S. Rubin, E. Rumbaugh, L. Saenz, M. R. Salvaggio, W. C. Sanchez, V. M. Sanjana, S. Santiago, W. Schmidt, H. Schuitemaker, P. M. Sestak, P. Shalit, W. Shay, V. N. Shirvani, V. I. Silebi, J. M. Sizemore, Jr., P. R. Skolnik, M. Sokol-Anderson, J. M. Sosman, P. Stabile, J. T. Stapleton, S. Starrett, F. Stein, H. J. Stellbrink, F. L. Sterman, V. E. Stone, D. R. Stone, G. Tambussi, R. A. Taplitz, E. M. Tedaldi, A. Telenti, W. Theisen, R. Torres, L. Tosiello, C. Tremblay, M. A. Tribble, P. D. Trinh, A. Tsao, P. Ueda, A. Vaccaro, E. Valadas, T. J. Vanig, I. Vecino, V. M. Vega, W. Veikley, B. H. Wade, C. Walworth, C. Wanidworanun, D. J. Ward, D. A. Warner, R. D. Weber, D. Webster, S. Weis, D. A. Wheeler, D. J. White, E. Wilkins, A. Winston, C. G. Wlodaver, A. van't Wout, D. P. Wright, O. O. Yang, D. L. Yurdin, B. W. Zabukovic, K. C. Zachary, B. Zeeman, M. Zhao, The major genetic determinants of HIV-1 control affect HLA class I peptide presentation. *Science* **330**, 1551-1557 (2010).

26. D. R. Collins, M. J. Olatotse, Z. J. Racenet, U. Arshad, E. Cakan, G. D. Gaiha, K. L. Clayton, B. D. Walker, Expanded Antigen-Specific Elimination Assay to Measure Human CD8(+) T Cell Cytolytic Potential. *Curr Protoc* **4**, e1109 (2024).

27. S. A. Yukl, P. Kaiser, P. Kim, S. Telwatte, S. K. Joshi, M. Vu, H. Lampiris, J. K. Wong, HIV latency in isolated patient CD4(+) T cells may be due to blocks in HIV transcriptional elongation, completion, and splicing. *Sci Transl Med* **10**, (2018).

28. S. L. Gooneratne, R. J. Center, S. J. Kent, M. S. Parsons, Functional advantage of educated KIR2DL1(+) natural killer cells for anti-HIV-1 antibody-dependent activation. *Clin Exp Immunol* **184**, 101-109 (2016).

29. N. Q. Zhao, R. Pi, D. N. Nguyen, T. Ranganath, C. Seiler, S. Holmes, A. Marson, C. A. Blish, NKp30 and NKG2D contribute to natural killer recognition of HIV-infected cells. *bioRxiv*, (2024).

30. M. Charmoy, T. Wyss, M. Delorenzi, W. Held, PD-1(+) Tcf1(+) CD8(+) T cells from established chronic infection can form memory while retaining a stable imprint of persistent antigen exposure. *Cell Rep* **37**, 110010 (2021).

31. T. Sekine, A. Perez-Potti, S. Nguyen, J. B. Gorin, V. H. Wu, E. Gostick, S. Llewellyn-Lacey, Q. Hammer, S. Falck-Jones, S. Vangeti, M. Yu, A. Smed-Sorensen, A. Gaballa, M. Uhlin, J. K. Sandberg, C. Brander, P. Nowak, P. A. Goepfert, D. A. Price, M. R. Betts, M. Buggert, TOX is expressed by exhausted and polyfunctional human effector memory CD8(+) T cells. *Sci Immunol* **5**, (2020).

32. Z. Strongin, L. Raymond Marchand, C. Deleage, M. B. Pampena, M. A. Cardenas, C. M. Beusch, T. N. Hoang, E. A. Urban, M. Gourves, K. Nguyen, G. K. Tharp, S. Lapp, A. R. Rahmberg, J. Harper, P. M. Del Rio Estrada, M. Gonzalez-Navarro, F. Torres-Ruiz, Y. A. Luna-Villalobos, S. Avila-Rios, G. Reyes-Teran, R. Sekaly, G. Silvestri, D. A. Kulpa, A. Saez-Cirion, J. M. Brenchley, S. E. Bosinger, D. E. Gordon, M. R. Betts, H. T. Kissick, M. Paiardini, Distinct SIV-specific CD8(+) T cells in the lymph node exhibit simultaneous effector and stem-like profiles and are associated with limited SIV persistence. *Nat Immunol* **25**, 1245-1256 (2024).

33. D. Zehn, R. Thimme, E. Lugli, G. P. de Almeida, A. Oxenius, 'Stem-like' precursors are the fount to sustain persistent CD8(+) T cell responses. *Nat Immunol* **23**, 836-847 (2022).
34. W. H. Hudson, J. Gensheimer, M. Hashimoto, A. Wieland, R. M. Valanparambil, P. Li, J. X. Lin, B. T. Konieczny, S. J. Im, G. J. Freeman, W. J. Leonard, H. T. Kissick, R. Ahmed, Proliferating Transitory T Cells with an Effector-like Transcriptional Signature Emerge from PD-1(+) Stem-like CD8(+) T Cells during Chronic Infection. *Immunity* **51**, 1043-1058 e1044 (2019).
35. J. A. Warren, S. Zhou, Y. Xu, M. J. Moeser, D. R. MacMillan, O. Council, J. Kirchherr, J. M. Sung, N. R. Roan, A. A. Adimora, S. Joseph, J. D. Kuruc, C. L. Gay, D. M. Margolis, N. Archin, Z. L. Brumme, R. Swanstrom, N. Goonetilleke, The HIV-1 latent reservoir is largely sensitive to circulating T cells. *Elife* **9**, (2020).
36. L. Shan, K. Deng, N. S. Shroff, C. M. Durand, S. A. Rabi, H. C. Yang, H. Zhang, J. B. Margolick, J. N. Blankson, R. F. Siliciano, Stimulation of HIV-1-specific cytolytic T lymphocytes facilitates elimination of latent viral reservoir after virus reactivation. *Immunity* **36**, 491-501 (2012).
37. C. L. Day, D. E. Kaufmann, P. Kiepiela, J. A. Brown, E. S. Moodley, S. Reddy, E. W. Mackey, J. D. Miller, A. J. Leslie, C. DePierres, Z. Mncube, J. Duraiswamy, B. Zhu, Q. Eichbaum, M. Altfeld, E. J. Wherry, H. M. Coovadia, P. J. Goulder, P. Klenerman, R. Ahmed, G. J. Freeman, B. D. Walker, PD-1 expression on HIV-specific T cells is associated with T-cell exhaustion and disease progression. *Nature* **443**, 350-354 (2006).
38. P. Tonnerre, D. Wolski, S. Subudhi, J. Aljabban, R. C. Hoogeveen, M. Damasio, H. K. Drescher, L. M. Bartsch, D. C. Tully, D. R. Sen, D. J. Bean, J. Brown, A. Torres-Cornejo, M. Robidoux, D. Kvistad, N. Alatrakchi, A. Cui, D. Lieb, J. A. Cheney, J. Gustafson, L. L. Lewis-Ximenez, L. Massenet-Regad, T. Eisenhaure, J. Aneja, W. N. Haining, R. T. Chung, N. Hacohen, T. M. Allen, A. Y. Kim, G. M. Lauer, Differentiation of exhausted CD8(+) T cells after termination of chronic antigen stimulation stops short of achieving functional T cell memory. *Nat Immunol* **22**, 1030-1041 (2021).
39. M. Rehr, J. Cahenzli, A. Haas, D. A. Price, E. Gostick, M. Huber, U. Karrer, A. Oxenius, Emergence of polyfunctional CD8+ T cells after prolonged suppression of human immunodeficiency virus replication by antiretroviral therapy. *J Virol* **82**, 3391-3404 (2008).
40. G. E. Martin, M. Pace, F. M. Shearer, E. Zilber, J. Hurst, J. Meyerowitz, J. P. Thornhill, J. Lwanga, H. Brown, N. Robinson, E. Hopkins, N. Olejniczak, N. Nwokolo, J. Fox, S. Fidler, C. B. Willberg, J. Frater, Levels of Human Immunodeficiency Virus DNA Are Determined Before ART Initiation and Linked to CD8 T-Cell Activation and Memory Expansion. *J Infect Dis* **221**, 1135-1145 (2020).
41. H. Takata, J. L. Mitchell, J. Pacheco, A. Pagliuzza, S. Pinyakorn, S. Buranapraditkun, C. Sacdalan, L. Leyre, S. Nathanson, J. C. Kakazu, J. Intasan, P. Prueksakaew, N. Chomchey, N. Phanuphak, M. de Souza, E. K. Haddad, M. Rolland, S. Tovanabutra, S. Vasan, D. C. Hsu, N. Chomont, L. Trautmann, Rv254/Search, Rv304/Search, An active HIV reservoir during ART is associated with maintenance of HIV-specific CD8(+) T cell magnitude and short-lived differentiation status. *Cell Host Microbe* **31**, 1494-1506 e1494 (2023).
42. C. Passaes, D. Desjardins, A. Chapel, V. Monceaux, J. Lemaitre, A. Melard, F. Perdomo-Celis, C. Planchais, M. Gourves, N. Dimant, A. David, N. Dereuddre-Bosquet, A. Barrail-Tran, H. Gouget, C. Guillaume, F. Relouzat, O. Lambotte, J. Guedj, M. Muller-Trutwin, H. Mouquet, C. Rouzioux, V. Avettand-Fenoel, R. Le Grand, A. Saez-Cirion, Early antiretroviral therapy favors post-treatment SIV control associated with the expansion of enhanced memory CD8(+) T-cells. *Nat Commun* **15**, 178 (2024).
43. M. Altfeld, J. van Lunzen, N. Frahm, X. G. Yu, C. Schneider, R. L. Eldridge, M. E. Feeney, D. Meyer-Olson, H. J. Stellbrink, B. D. Walker, Expansion of pre-existing, lymph node-localized CD8+ T cells during supervised treatment interruptions in chronic HIV-1 infection. *J Clin Invest* **109**, 837-843 (2002).

44. G. M. Ortiz, M. Wellons, J. Brancato, H. T. Vo, R. L. Zinn, D. E. Clarkson, K. Van Loon, S. Bonhoeffer, G. D. Miralles, D. Montefiori, J. A. Bartlett, D. F. Nixon, Structured antiretroviral treatment interruptions in chronically HIV-1-infected subjects. *Proc Natl Acad Sci U S A* **98**, 13288-13293 (2001).
45. E. S. Rosenberg, M. Altfeld, S. H. Poon, M. N. Phillips, B. M. Wilkes, R. L. Eldridge, G. K. Robbins, R. T. D'Aquila, P. J. Goulder, B. D. Walker, Immune control of HIV-1 after early treatment of acute infection. *Nature* **407**, 523-526 (2000).
46. E. H. Graf, M. J. Pace, B. A. Peterson, L. J. Lynch, S. B. Chukwulebe, A. M. Mexas, F. Shaheen, J. N. Martin, S. G. Deeks, M. Connors, S. A. Migueles, U. O'Doherty, Gag-positive reservoir cells are susceptible to HIV-specific cytotoxic T lymphocyte mediated clearance in vitro and can be detected in vivo [corrected]. *PLoS One* **8**, e71879 (2013).
47. S. H. Huang, Y. Ren, A. S. Thomas, D. Chan, S. Mueller, A. R. Ward, S. Patel, C. M. Bollard, C. R. Cruz, S. Karandish, R. Truong, A. B. Macedo, A. Bosque, C. Kovacs, E. Benko, A. Piechocka-Trocha, H. Wong, E. Jeng, D. F. Nixon, Y. C. Ho, R. F. Siliciano, B. D. Walker, R. B. Jones, Latent HIV reservoirs exhibit inherent resistance to elimination by CD8+ T cells. *J Clin Invest* **128**, 876-889 (2018).
48. W. Sun, C. Gao, C. A. Hartana, M. R. Osborn, K. B. Einkauf, X. Lian, B. Bone, N. Bonheur, T. W. Chun, E. S. Rosenberg, B. D. Walker, X. G. Yu, M. Lichterfeld, Phenotypic signatures of immune selection in HIV-1 reservoir cells. *Nature* **614**, 309-317 (2023).
49. R. T. Veenhuis, A. K. Kwaa, C. C. Garliss, R. Latanich, M. Salgado, C. W. Pohlmeyer, C. L. Nobles, J. Gregg, E. P. Scully, J. R. Bailey, F. D. Bushman, J. N. Blankson, Long-term remission despite clonal expansion of replication-competent HIV-1 isolates. *JCI Insight* **3**, (2018).
50. R. A. Pollack, R. B. Jones, M. Pertea, K. M. Bruner, A. R. Martin, A. S. Thomas, A. A. Capoferri, S. A. Beg, S. H. Huang, S. Karandish, H. Hao, E. Halper-Stromberg, P. C. Yong, C. Kovacs, E. Benko, R. F. Siliciano, Y. C. Ho, Defective HIV-1 Proviruses Are Expressed and Can Be Recognized by Cytotoxic T Lymphocytes, which Shape the Proviral Landscape. *Cell Host Microbe* **21**, 494-506 e494 (2017).
51. A. Samri, C. Bacchus-Souffan, L. Hocqueloux, V. Avettand-Fenoel, B. Descours, I. Theodorou, M. Larsen, A. Saez-Cirion, C. Rouzioux, B. Autran, A. V. s. group, Polyfunctional HIV-specific T cells in Post-Treatment Controllers. *AIDS* **30**, 2299-2302 (2016).
52. E. Esmaeilzadeh, B. Etemad, C. L. Lavine, L. Garneau, Y. Li, J. Regan, C. Wong, R. Sharaf, E. Connick, P. Volberding, M. Sagar, M. S. Seaman, J. Z. Li, Autologous neutralizing antibodies increase with early antiretroviral therapy and shape HIV rebound after treatment interruption. *Sci Transl Med* **15**, eabq4490 (2023).
53. J. Blazkova, F. Gao, M. H. Marichannegowda, J. S. Justement, V. Shi, E. J. Whitehead, R. F. Schneck, E. D. Huiting, K. Gittens, M. Cottrell, E. Benko, C. Kovacs, J. Lack, M. C. Sneller, S. Moir, A. S. Fauci, T. W. Chun, Distinct mechanisms of long-term virologic control in two HIV-infected individuals after treatment interruption of anti-retroviral therapy. *Nat Med* **27**, 1893-1898 (2021).
54. B. Etemad, X. Sun, Y. Li, M. Melberg, D. Moisi, R. Gottlieb, H. Ahmed, E. Aga, R. J. Bosch, E. P. Acosta, Y. Yuki, M. P. Martin, M. Carrington, R. T. Gandhi, J. M. Jacobson, P. Volberding, E. Connick, R. Mitsuyasu, I. Frank, M. Saag, J. J. Eron, D. Skiest, D. M. Margolis, D. Havlir, R. T. Schooley, M. M. Lederman, X. G. Yu, J. Z. Li, HIV post-treatment controllers have distinct immunological and virological features. *Proc Natl Acad Sci U S A* **120**, e2218960120 (2023).
55. M. Alexandre, M. Prague, E. Lhomme, J. D. Lelievre, L. Wittkop, L. Richert, Y. Levy, R. Thiebaut, Definition of Virological Endpoints Improving the Design of Human Immunodeficiency Virus (HIV) Cure Strategies Using Analytical Antiretroviral Treatment Interruption. *Clin Infect Dis*, (2024).

56. A. A. Okoye, D. D. Duell, Y. Fukazawa, B. Varco-Merth, A. Marenco, H. Behrens, M. Chaunzwa, A. N. Selseth, R. M. Gilbride, J. Shao, P. T. Edlefsen, R. Geleziunas, M. Pinkevych, M. P. Davenport, K. Busman-Sahay, M. Nekorchuk, H. Park, J. Smedley, M. K. Axthelm, J. D. Estes, S. G. Hansen, B. F. Keele, J. D. Lifson, L. J. Picker, CD8+ T cells fail to limit SIV reactivation following ART withdrawal until after viral amplification. *J Clin Invest* **131**, (2021).
57. B. Julg, L. Dee, J. Ananworanich, D. H. Barouch, K. Bar, M. Caskey, D. J. Colby, L. Dawson, K. L. Dong, K. Dube, J. Eron, J. Frater, R. T. Gandhi, R. Geleziunas, P. Goulder, G. J. Hanna, R. Jefferys, R. Johnston, D. Kuritzkes, J. Z. Li, U. Likhitwonnawut, J. van Lunzen, J. Martinez-Picado, V. Miller, L. J. Montaner, D. F. Nixon, D. Palm, G. Pantaleo, H. Peay, D. Persaud, J. Salzwedel, K. Salzwedel, T. Schacker, V. Sheikh, O. S. Sogaard, S. Spudich, K. Stephenson, J. Sugarman, J. Taylor, P. Tebas, C. T. Tiemessen, R. Tressler, C. D. Weiss, L. Zheng, M. L. Robb, N. L. Michael, J. W. Mellors, S. G. Deeks, B. D. Walker, Recommendations for analytical antiretroviral treatment interruptions in HIV research trials-report of a consensus meeting. *Lancet HIV* **6**, e259-e268 (2019).
58. Y. Nishimura, R. Gautam, T. W. Chun, R. Sadjadpour, K. E. Foulds, M. Shingai, F. Klein, A. Gazumyan, J. Golijanin, M. Donaldson, O. K. Donau, R. J. Plishka, A. Buckler-White, M. S. Seaman, J. D. Lifson, R. A. Koup, A. S. Fauci, M. C. Nussenzweig, M. A. Martin, Early antibody therapy can induce long-lasting immunity to SHIV. *Nature* **543**, 559-563 (2017).
59. P. Mendoza, H. Gruell, L. Nogueira, J. A. Pai, A. L. Butler, K. Millard, C. Lehmann, I. Suarez, T. Y. Oliveira, J. C. C. Lorenzi, Y. Z. Cohen, C. Wyen, T. Kummerle, T. Karagounis, C. L. Lu, L. Handl, C. Unson-O'Brien, R. Patel, C. Ruping, M. Schlotz, M. Witmer-Pack, I. Shimeliovich, G. Kremer, E. Thomas, K. E. Seaton, J. Horowitz, A. P. West, Jr., P. J. Bjorkman, G. D. Tomaras, R. M. Gulick, N. Pfeifer, G. Fatkenheuer, M. S. Seaman, F. Klein, M. Caskey, M. C. Nussenzweig, Combination therapy with anti-HIV-1 antibodies maintains viral suppression. *Nature* **561**, 479-484 (2018).
60. C. Gaebler, L. Nogueira, E. Stoffel, T. Y. Oliveira, G. Breton, K. G. Millard, M. Turroja, A. Butler, V. Ramos, M. S. Seaman, J. D. Reeves, C. J. Petroupoulos, I. Shimeliovich, A. Gazumyan, C. S. Jiang, N. Jilg, J. F. Scheid, R. Gandhi, B. D. Walker, M. C. Sneller, A. Fauci, T. W. Chun, M. Caskey, M. C. Nussenzweig, Prolonged viral suppression with anti-HIV-1 antibody therapy. *Nature* **606**, 368-374 (2022).
61. J. D. Gunst, J. F. Hojen, M. H. Pahus, M. Rosas-Umbert, B. Stiksrud, J. H. McMahon, P. W. Denton, H. Nielsen, I. S. Johansen, T. Benfield, S. Leth, J. Gerstoft, L. Ostergaard, M. H. Schleimann, R. Olesen, H. Stovring, L. Vibholm, N. Weis, A. M. Dyrhol-Riise, K. B. H. Pedersen, J. S. Y. Lau, D. C. Copertino, Jr., N. Linden, T. T. Huynh, V. Ramos, R. B. Jones, S. R. Lewin, M. Tolstrup, T. A. Rasmussen, M. C. Nussenzweig, M. Caskey, D. H. Reikvam, O. S. Sogaard, Impact of a TLR9 agonist and broadly neutralizing antibodies on HIV-1 persistence: the randomized phase 2a TITAN trial. *Nat Med* **29**, 2547-2558 (2023).
62. J. D. Gunst, M. H. Pahus, M. Rosas-Umbert, I. N. Lu, T. Benfield, H. Nielsen, I. S. Johansen, R. Mohey, L. Ostergaard, V. Klastrup, M. Khan, M. H. Schleimann, R. Olesen, H. Stovring, P. W. Denton, N. N. Kinloch, D. C. Copertino, A. R. Ward, W. D. C. Alberto, S. D. Nielsen, M. C. Puertas, V. Ramos, J. D. Reeves, C. J. Petropoulos, J. Martinez-Picado, Z. L. Brumme, R. B. Jones, J. Fox, M. Tolstrup, M. C. Nussenzweig, M. Caskey, S. Fidler, O. S. Sogaard, Early intervention with 3BNC117 and romidepsin at antiretroviral treatment initiation in people with HIV-1: a phase 1b/2a, randomized trial. *Nat Med* **28**, 2424-2435 (2022).
63. J. Niessl, A. E. Baxter, P. Mendoza, M. Jankovic, Y. Z. Cohen, A. L. Butler, C. L. Lu, M. Dube, I. Shimeliovich, H. Gruell, F. Klein, M. Caskey, M. C. Nussenzweig, D. E. Kaufmann, Combination anti-HIV-1 antibody therapy is associated with increased virus-specific T cell immunity. *Nat Med* **26**, 222-227 (2020).
64. M. Rosas-Umbert, J. D. Gunst, M. H. Pahus, R. Olesen, M. Schleimann, P. W. Denton, V. Ramos, A. Ward, N. N. Kinloch, D. C. Copertino, T. Escriba, A. Llano, Z. L. Brumme, R. Brad Jones, B.

Mothe, C. Brander, J. Fox, M. C. Nussenzweig, S. Fidler, M. Caskey, M. Tolstrup, O. S. Sogaard, Administration of broadly neutralizing anti-HIV-1 antibodies at ART initiation maintains long-term CD8(+) T cell immunity. *Nat Commun* **13**, 6473 (2022).

65. S. Y. Lim, J. Lee, C. E. Osuna, P. Vikhe, D. R. Schalk, E. Chen, E. Fray, M. Kumar, N. Schultz-Darken, E. Rakasz, S. Capuano, R. A. Ladd, H. M. Gil, D. T. Evans, E. K. Jeng, M. Seaman, M. Martin, C. Van Dorp, A. S. Perelson, H. C. Wong, J. D. Siliciano, R. Siliciano, J. T. Safrit, D. F. Nixon, P. Soon-Shiong, M. Nussenzweig, J. B. Whitney, Induction of durable remission by dual immunotherapy in SHIV-infected ART-suppressed macaques. *Science* **383**, 1104-1111 (2024).
66. D. C. Tully, C. B. Ogilvie, R. E. Batorsky, D. J. Bean, K. A. Power, M. Ghebremichael, H. E. Bedard, A. D. Gladden, A. M. Seese, M. A. Amero, K. Lane, G. McGrath, S. B. Bazner, J. Tinsley, N. J. Lennon, M. R. Henn, Z. L. Brumme, P. J. Norris, E. S. Rosenberg, K. H. Mayer, H. Jessen, S. L. Kosakovsky Pond, B. D. Walker, M. Altfeld, J. M. Carlson, T. M. Allen, Differences in the Selection Bottleneck between Modes of Sexual Transmission Influence the Genetic Composition of the HIV-1 Founder Virus. *PLoS Pathog* **12**, e1005619 (2016).
67. H. Zhang, Y. Zhou, C. Alcock, T. Kiefer, D. Monie, J. Siliciano, Q. Li, P. Pham, J. Cofrancesco, D. Persaud, R. F. Siliciano, Novel single-cell-level phenotypic assay for residual drug susceptibility and reduced replication capacity of drug-resistant human immunodeficiency virus type 1. *J Virol* **78**, 1718-1729 (2004).
68. M. S. Malnati, G. Scarlatti, F. Gatto, F. Salvatori, G. Cassina, T. Rutigliano, R. Volpi, P. Lusso, A universal real-time PCR assay for the quantification of group-M HIV-1 proviral load. *Nature protocols* **3**, 1240-1248 (2008).
69. G. M. Laird, C. K. Bullen, D. I. Rosenbloom, A. R. Martin, A. L. Hill, C. M. Durand, J. D. Siliciano, R. F. Siliciano, Ex vivo analysis identifies effective HIV-1 latency-reversing drug combinations. *The Journal of clinical investigation* **125**, 1901-1912 (2015).
70. N. A. J. Cassidy, C. S. Fish, C. N. Levy, P. Roychoudhury, D. B. Reeves, S. M. Hughes, J. T. Schiffer, S. Benki-Nugent, G. John-Stewart, D. Wamalwa, K. R. Jerome, J. Overbaugh, F. Hladik, D. A. Lehman, HIV reservoir quantification using cross-subtype multiplex ddPCR. *iScience* **25**, 103615 (2022).
71. C. S. Fish, N. A. J. Cassidy, C. N. Levy, S. M. Hughes, K. R. Jerome, J. Overbaugh, F. Hladik, D. A. Lehman, Protocol for high-throughput reservoir quantification across global HIV subtypes using a cross-subtype intact proviral DNA assay. *STAR Protoc* **3**, 101681 (2022).
72. C. Hafemeister, R. Satija, Normalization and variance stabilization of single-cell RNA-seq data using regularized negative binomial regression. *Genome Biol* **20**, 296 (2019).
73. Y. Hao, S. Hao, E. Andersen-Nissen, W. M. Mauck, 3rd, S. Zheng, A. Butler, M. J. Lee, A. J. Wilk, C. Darby, M. Zager, P. Hoffman, M. Stoeckius, E. Papalexi, E. P. Mimitou, J. Jain, A. Srivastava, T. Stuart, L. M. Fleming, B. Yeung, A. J. Rogers, J. M. McElrath, C. A. Blish, R. Gottardo, P. Smibert, R. Satija, Integrated analysis of multimodal single-cell data. *Cell* **184**, 3573-3587 e3529 (2021).
74. Q. Yang, K. R. Safina, K. D. Q. Nguyen, Z. K. Tuong, N. Borcherding, scRepertoire 2: Enhanced and efficient toolkit for single-cell immune profiling. *PLoS Comput Biol* **21**, e1012760 (2025).
75. T. Sundell, K. Grimstad, A. Camponeschi, A. Tilevik, I. Gjertsson, I. L. Martensson, Single-cell RNA sequencing analyses: interference by the genes that encode the B-cell and T-cell receptors. *Brief Funct Genomics* **22**, 263-273 (2022).
76. J. Zyla, M. Marczyk, T. Domaszewska, S. H. E. Kaufmann, J. Polanska, J. Weiner, Gene set enrichment for reproducible science: comparison of CERNO and eight other algorithms. *Bioinformatics* **35**, 5146-5154 (2019).
77. A. Subramanian, P. Tamayo, V. K. Mootha, S. Mukherjee, B. L. Ebert, M. A. Gillette, A. Paulovich, S. L. Pomeroy, T. R. Golub, E. S. Lander, J. P. Mesirov, Gene set enrichment analysis: a

knowledge-based approach for interpreting genome-wide expression profiles. *Proc Natl Acad Sci U S A* **102**, 15545-15550 (2005).
78. D. R. Collins, J. Hitschfel, J. M. Urbach, G. H. Mylvaganam, N. L. Ly, U. Arshad, Z. J. Racenet, A. G. Yanez, T. J. Diefenbach, B. D. Walker, Cytolytic CD8(+) T cells infiltrate germinal centers to limit ongoing HIV replication in spontaneous controller lymph nodes. *Sci Immunol* **8**, eade5872 (2023).

Acknowledgments: The authors are grateful to the study participants; to the American Red Cross HLA genotyping laboratory; and to Alicja Piechocka-Trocha, Ashok Khatri, Michael Waring, Karen Power, Fernando Senjobe, Nishant Singh, Julia Hitschfel, and Elif Çakan for technical advice and assistance.

Funding: This work was supported by funding from United States National Institutes of Health (NIH) R01 AI149704, R01 AI157854, R01 AI172843, DP2 AI184606, P01 AI169768, P30 AI042853, P30 AI060354, T32 AI007387, L30 AI126472, and Howard Hughes Medical Institute. This project was further supported by Clinical Translational Science Award 1UL1TR002541 to Harvard University and Brigham and Women's Hospital from the National Center for Research Resources. The content is solely the responsibility of the authors and does not necessarily represent the official views of the National Center for Research Resources or the National Institutes of Health. Funders had no role in study design, data collection and analysis, decision to publish or preparation of the manuscript.

Author contributions:
Conceptualization: DRC, AT
Methodology: DRC, LCW, KLC, MS, SZ, AT
Investigation: DRC, MJO, SZ, TJL, RR, XH, JYC, BC, UA, ZJR, HW, CC, XG, JMD
Data curation: HCJ, JMU, ZZ, NS, JB, DRC, AT
Formal analysis: EM, JMU, DRC, ZZ, NS, JB
Resources: SHS, BDW, AT
Writing – original draft: DRC
Writing – review and editing: All authors
Funding acquisition: DRC, BDW, MS, AT
Supervision: DRC, MS, SHS, BDW, AT

Competing interests: AT receives remuneration for editorial work performed at DynaMed, EBSCO. The remaining authors declare that no competing interests exist.

Data and materials availability: Single-cell multiomics are available via NCBI Gene Expression Omnibus (GEO) accession numbers pending and GSE294440. The remaining data are included in the manuscript and supplementary materials.

Figures:

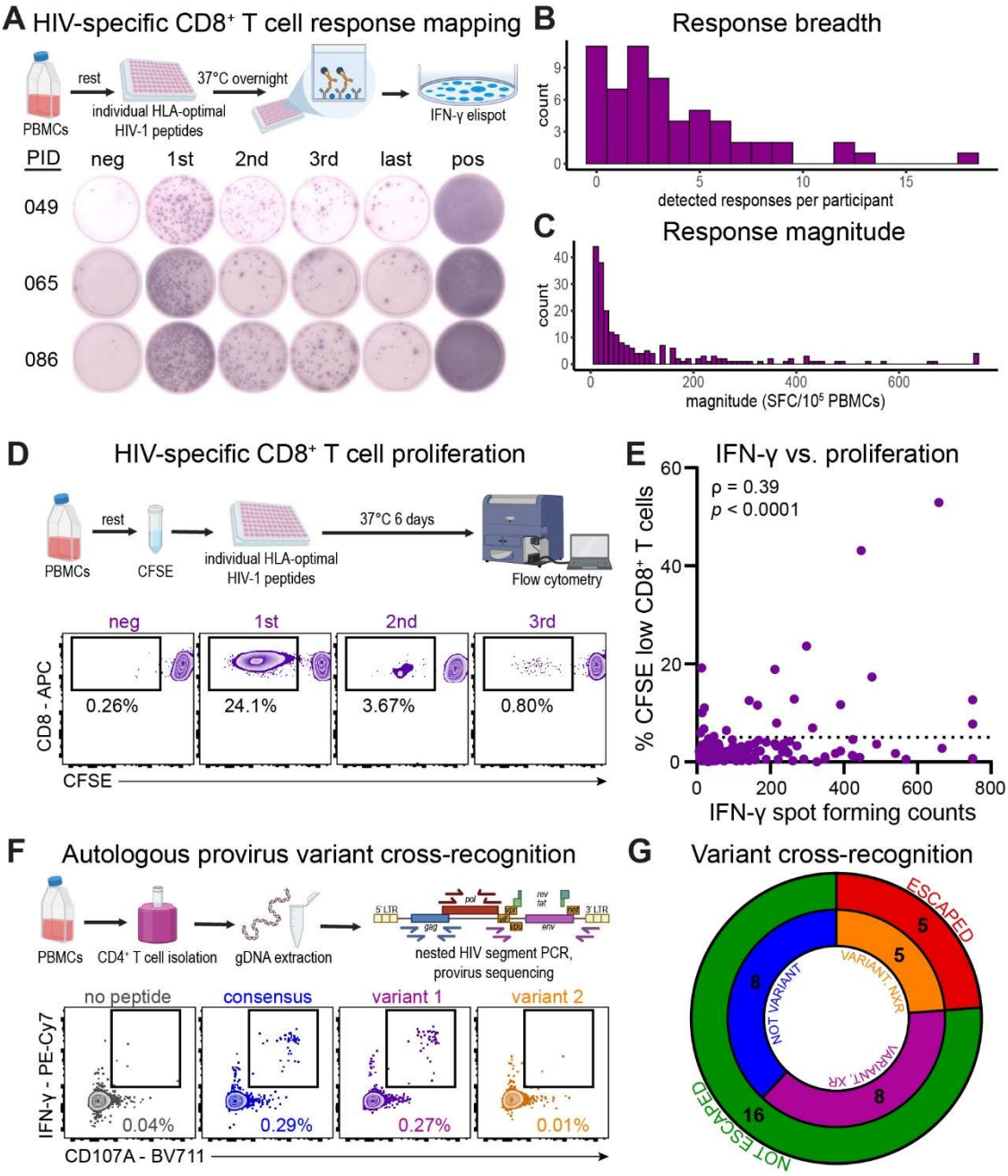

Fig. 1: HIV-specific CD8$^+$ T cell functionality against autologous proviral epitopes. (A) Schematic overview of HIV-specific CD8$^+$ T cell response mapping screen and representative interferon- γ (IFN-γ) elispot results from 3 participants. **(B)** Histogram of CD8$^+$ T cell response breadths measured by number of HLA-optimal HIV-1 epitopes eliciting IFN-γ elispot responses per participant (n=60). **(C)** Histogram of HIV-specific CD8$^+$ T cell response magnitudes measured by IFN-γ spot-forming counts (SFC) per 100,000 PBMCs for each detectable response against HLA-optimal HIV-1 epitopes (n=221). **(D)** Schematic overview of HIV-specific CD8$^+$ T cell proliferation assay and example results from the 3 largest responses detected by IFN- γ elispot in participant H003. **(E)** Summary of proliferation assay results across n=221 responses

(from 60 participants) detected above background by IFN-γ elispot and Spearman correlation (ρ) with IFN-γ magnitudes as measured in C. Dashed line represents 5% proliferation, above which proliferation results were confirmed by independent replicates following initial screening. **(F)** Schematic overview of HIV-1 provirus sequencing and example cross-recognition assay results from participant H075 targeting consensus and two autologous proviral B*07 Nef TM9 variants. **(G)** Doughnut plot of autologous proviral epitope variant cross-recognition and mutational escape across *n*=21 proliferative responses (from 16 participants) identified in E. XR, cross-recognized; NXR, not cross-recognized.

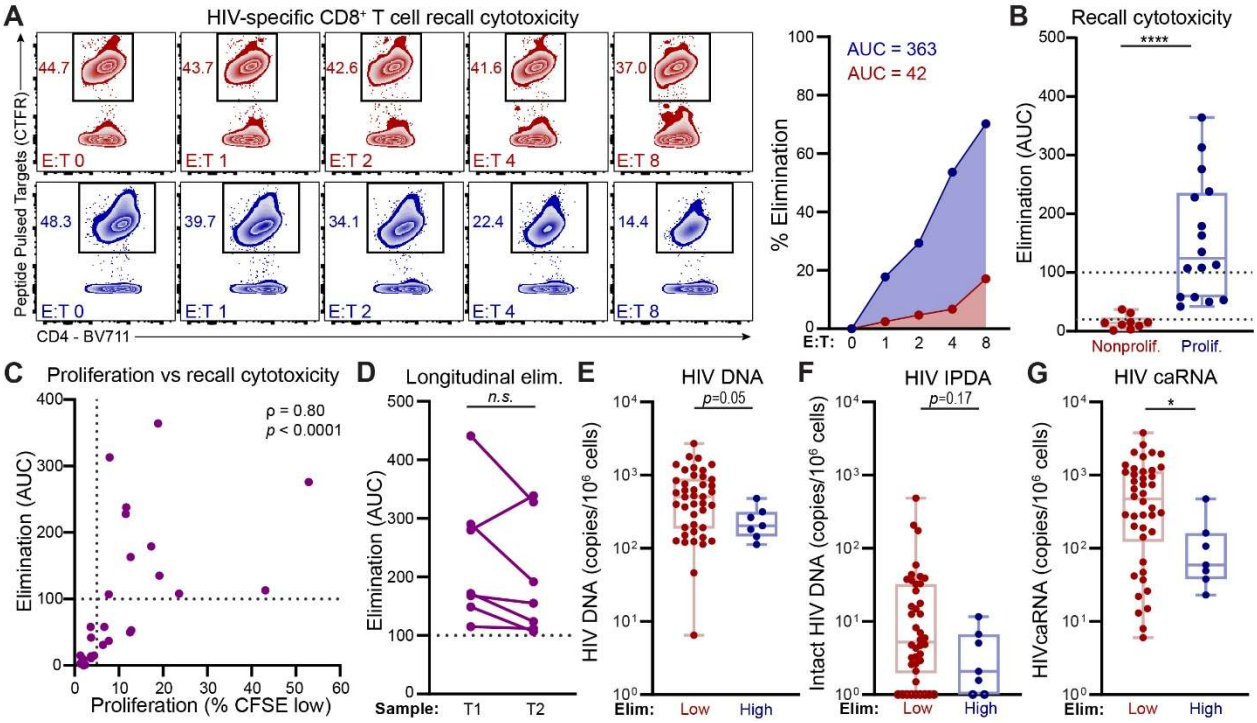

Fig. 2: HIV-specific CD8⁺ T cell cytolytic capacity is associated with HIV-1 reservoir suppression. (A) Left: Example frequencies of residual Gag TPQDLNTML peptide-pulsed target CD4⁺ T cells labeled with CellTrace Far Red (CTFR) after coculture with autologous peptide-expanded effector CD8⁺ T cells at increasing effector:target (E:T) ratios for two responses with high (blue) or low (red) proliferative capacities. Right: Percent elimination plotted across E:T ratios for representative elimination responses shown on left, with area-under-curve (AUC) summary values. **(B)** Summary of recall cytotoxicities across all proliferative (% CFSE low ≥5%, *n*=16 responses from 14 participants) and a sampling of immunodominant nonproliferative (% CFSE low < 5%, *n*=9 responses from 8 participants) HIV-1 epitope-specific responses. Dashed lines at AUC=100 and AUC=20 represent thresholds for classification of responses with high, moderate, and low cytolytic capacities. ****p<0.0001, Wilcoxon rank-sum test. **(C)** Spearman correlation (ρ) and corresponding correlation test of proliferative capacity measured by CFSE dilution assay versus recall cytotoxicity measured by expanded antigen-specific elimination assay (*n*=25 responses from 22 participants). Dashed lines at AUC=100 and 5% CFSE low represent thresholds for classification of responses with high cytolytic and proliferative capacities, respectively. **(D)** Recall cytotoxicity (elimination AUC) across longitudinal samples spanning 1-5 years in *n*=7 participants who had high recall cytotoxicity (AUC >100; *n.s.*, not significant; p=0.16, Wilcoxon matched-pairs signed rank test). **(E-G)**

Measurements of total HIV-1 proviral DNA (E), intact HIV-1 proviral DNA measured by the intact HIV-1 provirus assay (IPDA, F), and cell-associated HIV-1 RNA (caRNA, G) copies per 10^6 PBMCs from participants with HIV-specific $CD8^+$ T cell responses of low (max. elim AUC <100, *n*=42 participants) or high (max. elim AUC >100, *n*=7 participants) cytolytic capacity. Open circles at 10^0 represent values below the assay detection limit. *$p < 0.05$; *p*-values calculated by Wilcoxon rank-sum tests.

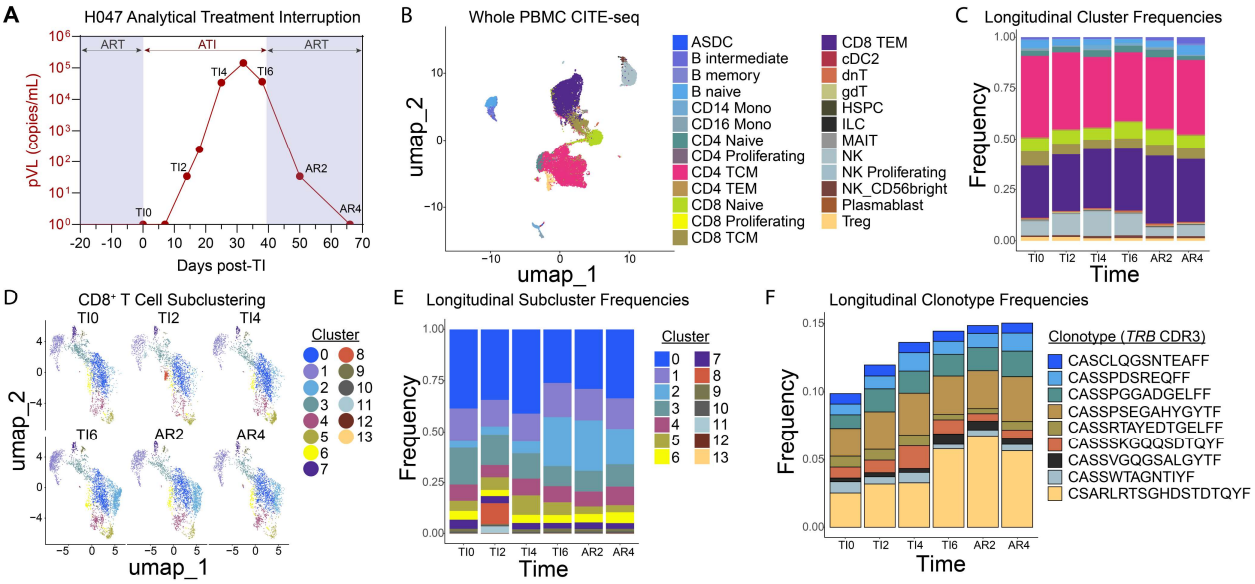

Fig. 3. **Interruption of antiretroviral therapy initiates sequential NK and clonal $CD8^+$ T cell expansions. (A)** Longitudinal plasma HIV-1 viral loads (pVL, $\log_{10}$ scale) monitored during ATI in H047. Unshaded region indicates beginning of ATI at day 0 (TI0) and resumption of ART following the sample collected on day 38 (TI6). Biweekly PBMC sample collections are labeled; TI, treatment interruption; AR, ART-restart; numbers represent weeks. **(B)** WNN analysis of a 5' CITE-seq dataset of PBMC and 154 surface proteins, displayed as a UMAP visualization. ASDC, AXL^+ $SIGLEC6^+$ dendritic cells; B intermediate, transitional/intermediate stage B cells; CD14 Mono, $CD14^+$ classical monocytes; CD16 Mono, $CD16^+$ nonclassical monocytes; TCM, central memory T cells; TEM, effector-memory T cells; cDC2, type-2 conventional dendritic cells; dnT, double-negative T cells ($CD4^-CD8^-$); gdT, γδ T cells; HSPC, hematopoietic stem and progenitor cells; ILC, innate lymphoid cells; MAIT, mucosal-associated invariant T cells; Treg, regulatory T cells. **(C)** Stacked bar plot of PBMC proportions over time **(D)** Longitudinal $CD8^+$ T cell sub-clustering at resolution 0.2 identifies expansion of cluster 2, most notable at TI6, that begins to contract by AR4. **(E)** Stacked bar plots of $CD8^+$ T cell subcluster frequencies from D at each ATI sample timepoint. **(F)** Stacked bar plots of $CD8^+$ T cell clonotype frequencies, as defined by complementary-determining region 3 (CDR3) sequence of the T cell receptor beta (*TRB*) chain and plotted as fractions of total $CD8^+$ T cells.

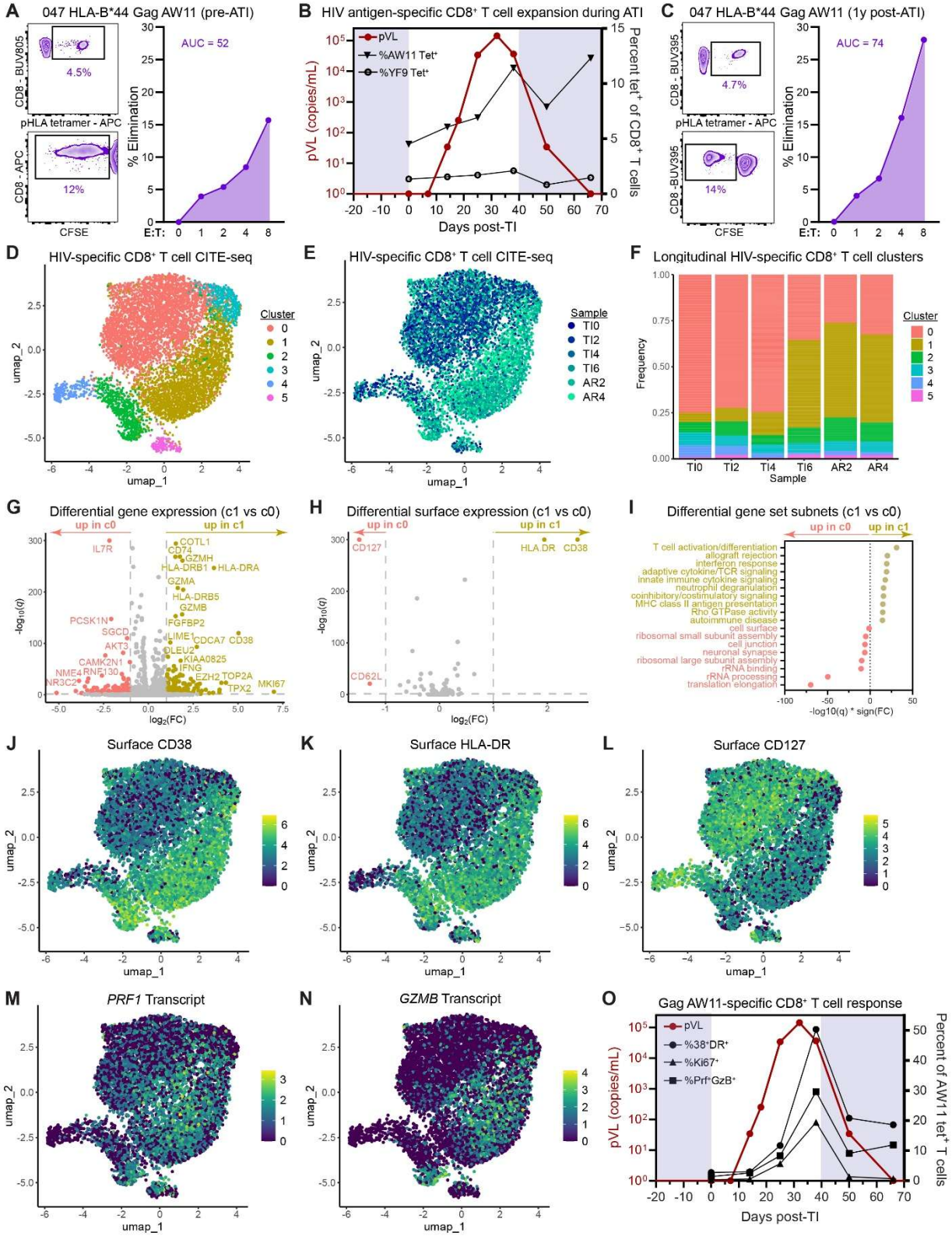

Fig. 4: *In vivo* HIV-specific CD8$^+$ T cell expansion and cytolytic effector differentiation accompany blunted rebound viremia during ATI. (A) Summary of HLA-B*44:02-restricted HIV-1 Gag AEQASQEVKNW (AW11) CD8$^+$ T cell response frequency (top left), proliferative

capacity (bottom left), and secondary cytolytic potential (right) in participant H047 prior to analytical treatment interruption (ATI). **(B)** Longitudinal plasma HIV-1 viral loads (pVL; left axis, $\log_{10}$ scale) monitored during ATI in H047. Unshaded region indicates beginning of ATI at day 0 and resumption of ART following the sample collected on day 38 (red circles). Immunodominant AW11-specific (black triangles), and subdominant Nef YF9-specific $CD8^+$ T cell frequencies measured by pHLA tetramer (Tet) staining during ATI in H047 (right axis, linear scale). **(C)** Summary of AW11-specific $CD8^+$ T cell response frequency (top left), proliferative capacity (bottom left), and secondary cytolytic potential (right) in participant H047 one year post-ATI. **(D-E)** UMAP projection of single-cell transcriptomes derived from AW11-specific $CD8^+$ T cells during ATI in participant H047, colored by shared nearest neighbor clustering (D) or by sample time-point (E). **(F)** Frequencies of clusters shown in D at each sample time-point during ATI. **(G-H)** Summary of differential gene (G) and surface marker (H) expression between clusters 0 and 1 among AW11-specific $CD8^+$ T cells. Dashed lines represent significance ($q<0.05$) and fold change (FC>2) thresholds. **(I)** Summary of the top significantly differential gene set subnets between cluster 0 and cluster 1 derived from gene set network analysis (GSNA). **(J-N)** UMAP projection of single-cell transcriptomes derived from AW11-specific $CD8^+$ T cells during ATI in H047, colored by log-normalized expression of surface CD38 (J), HLA-DR (K), CD127 (L), *PRF1* transcript (M), or *GZMB* transcript (N). **(O)** Longitudinal HIV-1 pVL (red circles, left axis, $\log_{10}$ scale), *in vivo* HIV-specific $CD8^+$ T cell activation measured by CD38 and HLA-DR co-expression (black circles, right axis, linear scale), proliferation measured by Ki-67 (black triangles, right axis, linear scale), and cytotoxic effector differentiation measured by perforin and granzyme B coexpression (black squares, right axis, linear scale) by flow cytometry among AW11 tet^+ $CD8^+$ T cells during ATI in H047.

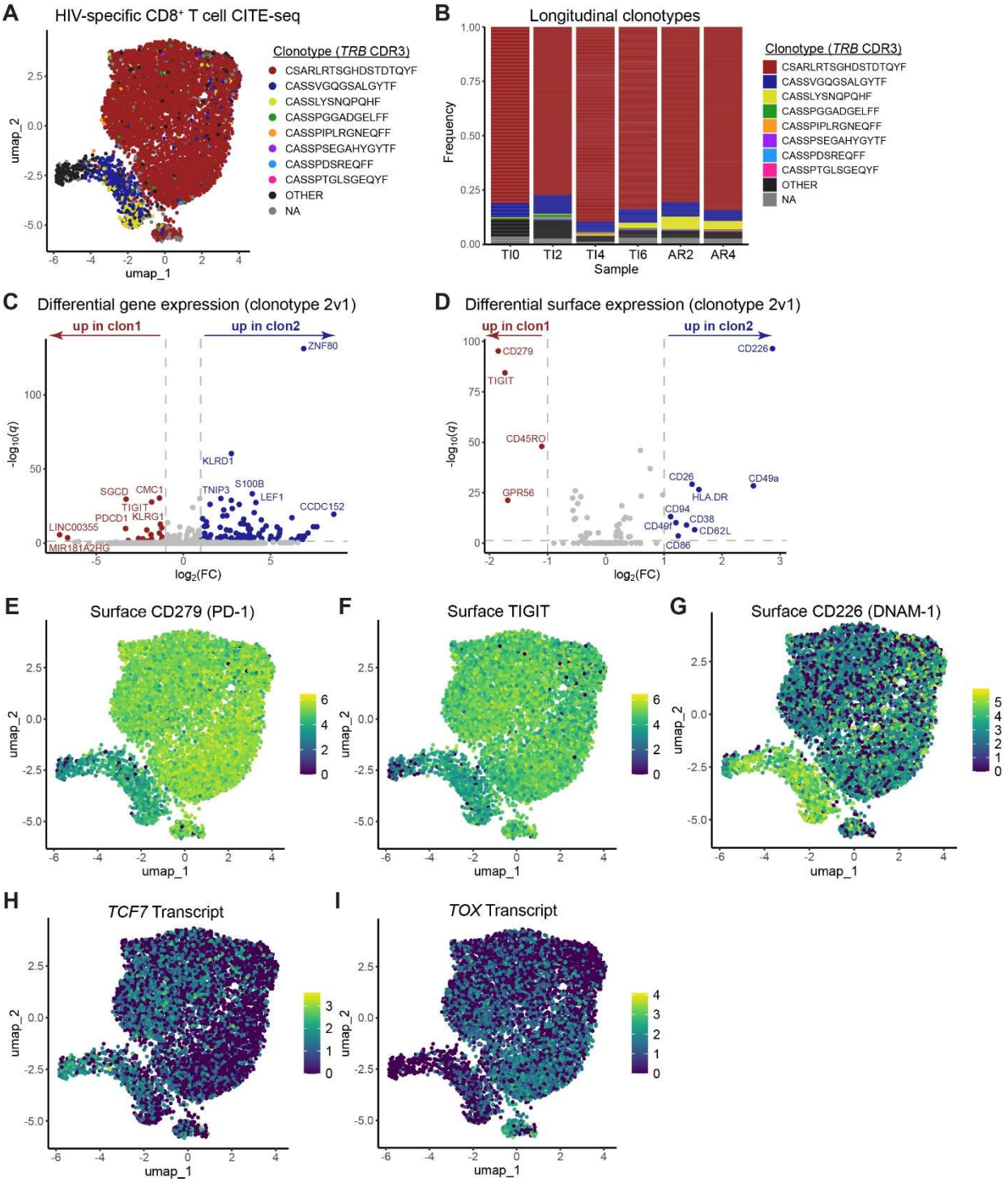

Fig. 5: Stem-like and quiescent memory T cell clonotypes expand in parallel during antiretroviral therapy interruption. (A) UMAP projection of single-cell transcriptomes derived from AW11-specific CD8$^+$ T cells during ATI in H047, colored by TCR clonotype and labeled by *TRB* CDR3 sequences. **(B)** Frequencies of clonotypes shown in A at each sample time-point during ATI. **(C-D)** Summary of differential gene (C) and surface marker (D) expression between clonotypes CSARLRTSGHDSTDTQYF (clon1) and CASSVGQGSALGYTF (clon2) among AW11-specific CD8$^+$ T cells. Dashed lines represent

significance (q<0.05) and fold change (FC>2) thresholds. **(E-I)** UMAP projection of single-cell transcriptomes derived from AW11-specific $CD8^+$ T cells during ATI in H047, colored by log-normalized expression of surface CD279/PD-1 (E), TIGIT (F), CD226 (G), *TCF7* transcript (H), or *TOX* transcript (I).

Table 1. Demographics and clinical characteristics of study participants.

Age at sampling (years; median, IQR)		54 (48–59)
Sex	Female (*n*, %)	23 (38.3%)
	Male (*n*, %)	37 (61.7%)
Race, Ethnicity	Asian, Not Hispanic (*n*, %)	1 (1.7%)
	Black, Hispanic (*n*, %)	2 (3.3%)
	Black, Not Hispanic (*n*, %)	19 (31.7%)
	Black, Unknown (*n*, %)	1 (1.7%)
	White, Hispanic (*n*, %)	7 (11.7%)
	White, Not Hispanic (*n*, %)	18 (30%)
	White, Unknown (*n*, %)	2 (3.3%)
	Other/Unknown, Hispanic (*n*, %)	10 (16.7%)
HIV-1 diagnosis to ART initiation interval (days; median, IQR)		42 (4–479)
ART initiation to sampling interval (years; median, IQR)		19 (11–22)
Peak plasma viral load ($\log_{10}$ HIV-1 RNA copies/ml; median, IQR)		4.9 (3.9–5.5)
Viral load at sampling (HIV-1 RNA copies/ml)		Undetectable (<20)
CD4 nadir (cells/mm^3; median, IQR)		202 (27–367)
CD4 count at sampling (cells/mm^3; median, IQR)		689 (511–913)